PATTERNS OF NATURAL AVALANCHE ACTIVITY ASSOCIATED WITH NEW

SNOW WATER EQUIVALANCE AND UPPER ATMOSPHERIC WIND DIRECTION

AND SPEED IN THE MOUNTAINS SURROUNDING GOTHIC, COLORADO

by

Tara Lea Chesley-Preston

A thesis submitted in partial fulfillment
of the requirements for the degree

of

Master of Science

in

Earth Sciences

MONTANA STATE UNIVERSITY
Bozeman, Montana

May, 2010

APPROVAL

of a thesis submitted by

Tara Lea Chesley-Preston

This thesis has been read by each member of the thesis committee and has been found to be satisfactory regarding content, English usage, format, citation, bibliographic style, and consistency and is ready for submission to the Division of Graduate Education.

Dr. Stephan G. Custer
(Co-Chair)

Dr. Karl W. Birkeland
(Co-Chair)

Approved for the Department of Earth Sciences

Dr. Stephan G. Custer

Approved for the Division of Graduate Education

Dr. Carl A. Fox

STATEMENT OF PERMISSION TO USE

Tara Lea Chesley-Preston

May, 2010

ACKNOWLEDGEMENTS

TABLE OF CONTENTS

Table of Contents - Continued

LIST OF TABLES

LIST OF TABLES - CONTINUED

LIST OF FIGURES

LIST OF FIGURES

ABSTRACT

Snowfall, temperature and wind are three factors that quickly change avalanche conditions. Ridge-top winds have been used to assess avalanche conditions with mixed success due to high variability. Few analyses have tested the effect upper atmospheric winds have on avalanche conditions. This study attempts to quantify the effect upper atmospheric wind direction and speed have on the spatial pattern of natural avalanching in the mountains near Gothic, Colorado. The Gothic dataset consists of over 3,300 natural avalanches spanning a time period of 33 years. These data are associated with daily new snow water equivalence (SWE) collected at Gothic, as well as 500mb wind direction and speed from the National Centers for Environmental Protection/National Center for Atmospheric Research (NCEP/NCAR) gridded reanalysis project. I hypothesize that prevailing 500mb winds are more likely to be associated with natural avalanches in avalanche paths with a starting zone aspect lee to the prevailing free air winds. In addition, I hypothesize that the odds of a natural avalanche occurring increases with increasing new SWE, increasing 500mb wind speeds, and 500mb wind direction. These hypotheses are tested using simple probability analysis as well as a two-component hurdle model.

As expected, avalanche paths lee to the 500mb wind direction have an increased probability of avalanching in relation to paths facing in other directions. However, exceptions do occur, some of which can be explained by cross-loading. The hurdle model results indicate that after accounting for new SWE, 500mb wind speed is significant in determining whether or not a day will be considered an avalanche day. Once a day is determined to be an avalanche day, 500mb wind direction is an important determinant for the daily avalanche hazard after accounting for new SWE. These results have practical significance. They give avalanche forecasters confidence that upper air wind direction is a useful predictor of the pattern of avalanche activity at the valley or mountain range scale, and the exceptions observed show that such predictions cannot be applied at the path scale. These scale issues demonstrate the general nature of backcountry advisories and why they cannot be applied at the scale of individual slopes.

INTRODUCTION

The need for accurate and timely avalanche forecasting is growing with the increase in winter backcountry use and travel (McClung 2002a; 2002b). While the understanding and experience of a human forecaster can never be replaced, there is still need for more quantitative forecasting tools and information. Increasingly, ski areas, helicopter operations, transportation departments, and avalanche centers are collecting detailed records of both natural and human triggered avalanches. Many different individuals record these events, each using slightly different methods and techniques. Rarely does one individual collect and record all of the observations, and even more atypical is to have a dataset outside a ski area that reports natural avalanches not impacted by backcountry recreationists or avalanche control. Therefore the Gothic, Colorado avalanche record, where natural avalanche events have been recorded by a single individual since the winter season of 1975-1976, is extremely unique and as far as I am aware the only record of its kind in the world. New snowfall, wind, and terrain combine to contribute to the formation of slab avalanches but their interaction is rarely quantified (McCollister, 2004). This research utilizes the Gothic dataset to better understand factors associated with the occurrence of natural avalanches around the Gothic, Colorado area. Ultimately the goal of this research is to describe the effects and interactions of new snowfall, upper atmospheric free air wind speed and direction, and their interaction with terrain and natural avalanche activity in the mountains surrounding Gothic, Colorado.

Gothic, Colorado, is a ghost town approximately 4 miles north of Mount Crested Butte Ski Area in the Elk Mountains of central Colorado (Fig. 1). Today Gothic is home to the Rocky Mountain Biological Laboratory (RMBL). RMBL is primarily a seasonal outdoor laboratory but has caretakers that reside in the valley throughout the entire year. In the winter of 1975-1976 Art Mears began collecting avalanche data at Gothic with the standard U.S. method (Perla and Martinelli, 1978, p. 225). The following season the data collection was turned over to a trained seasonal caretaker, billy barr, who continues the avalanche data collection to this day. The dataset contains 99.9% naturally triggered avalanches, making it the only known avalanche dataset of its kind in the world. Due to the fact that the road is closed to motorized use in the winter, outdoor enthusiasts have only recently begun venturing into the valley and triggering avalanches. Therefore knowledge about factors that control avalanche hazard in this area is becoming increasingly important.

Gothic is in a continental climate zone, far from a major water source, with cold air temperatures (averaging -7° C), a shallow snowpack (averaging a 110 cm deep snowpack), and very light, fluffy new snow (average density of 70 kg/m^3) (Armstrong and Armstrong, 1987; Mock and Kay, 1992; Mock and Birkeland, 2000; McClung and Schaerer, 2006). The town site of Gothic is approximately 2890 m above sea level at a latitude of 38° 57' 19.60" N and longitude of 106° 59' 28.32" W. The mean annual snowfall at Gothic is 1101 cm and the month that averages the most snowfall is February with 177.4 cm of snow. The average yearly snow water equivalent (SWE) is 69.95 cm (RMBL, 2009).
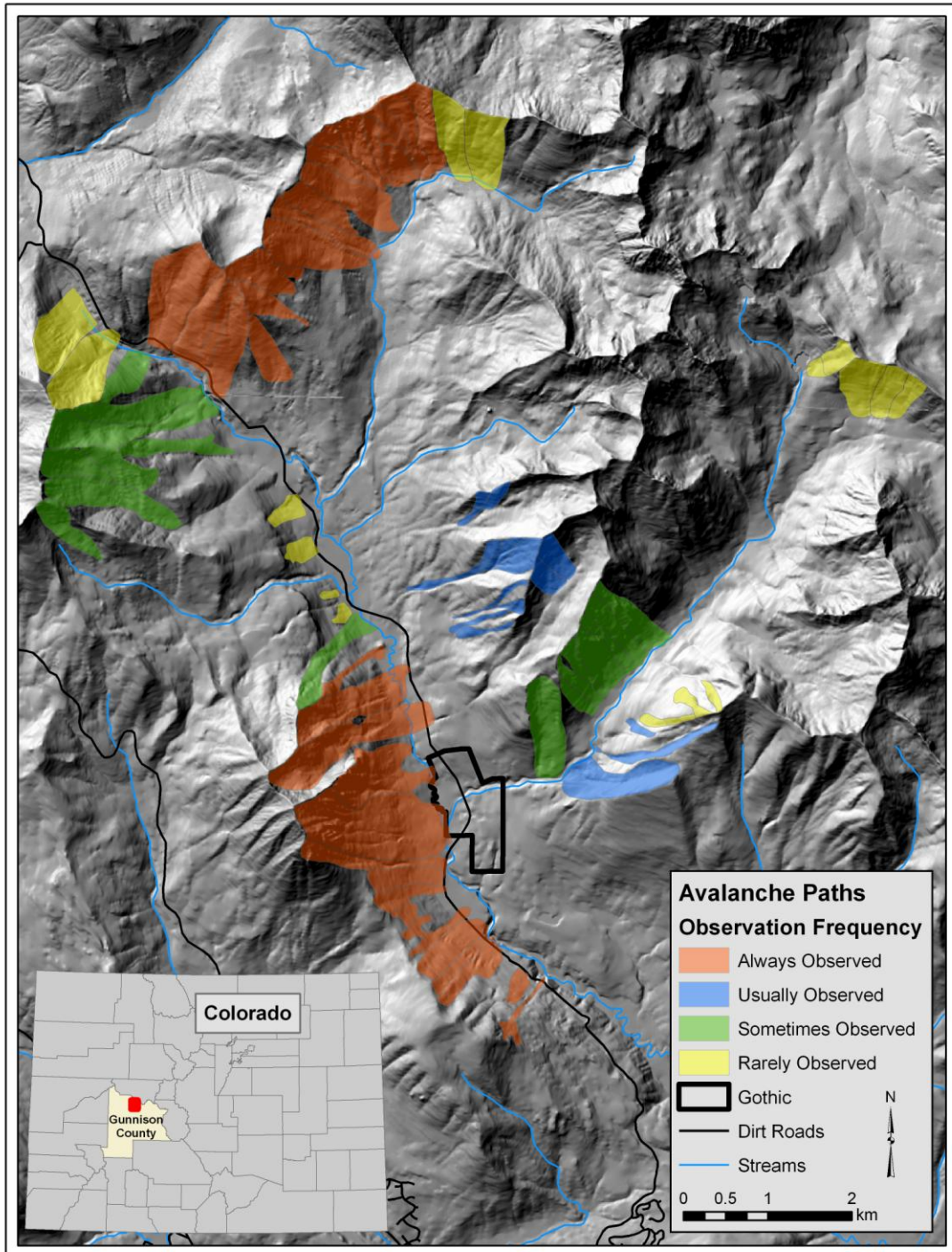
Figure 1: Study area location along with avalanche paths surrounding Gothic, Colorado and their observational frequency.

Weather has been correlated to avalanches through many modeling and observational studies (Fitzharris, 1981; Buser, 1983; Fitzharris, 1987; Mock and Kay, 1992; Glazovskaya, 1998; Mock and Birkeland, 2000; Brabec and Meister, 2001; Hageli and McClung, 2003; Hebertson and Jenkins, 2003; McCollister et al., 2003; McCollister, 2004; Haegeli and McClung, 2007). New snowfall, wind speed, and wind direction are all major weather factors contributing to avalanche formation (Buser et al., 1985). Avalanche activity increases with snow loading, whether it is via new snowfall or the interaction of wind and terrain, which influences the redistribution of snow by wind (McCollister, 2004; Morrison, 2004). The single best variable for avalanche prediction is 24-hour new snow depth but this factor does not explain all of the variability within avalanche prediction (Buser et al., 1985; Bakkehøi, 1986; Birkeland et al., 2001, McCollister, 2004). Most of the previous studies have been conducted in areas with artificially triggered avalanches (i.e., Hageli and McClung, 2003; McCollister, 2004). These studies have all included artificially triggered avalanches in the subsequent analyses; therefore they provide incomplete information regarding the natural avalanche system so important to backcountry avalanche forecasters and recreationists.

Many different computer aided and statistical approaches have been assembled to assist avalanche forecasters and ski patrols in their daily avalanche hazard assessment. Buser (1983; 1989) found that many statistical methods were too complex to actually be useful tools in avalanche forecasting. Therefore, he created a nearest neighbor approach which allows the forecaster to base decisions upon the avalanche conditions of the 20 most similar days. Similar approaches have proven to be quite useful for small scale

forecasting operations (Buser, 1989; Brabec and Meister, 2001; Purves et al., 2003; McCollister et al., 2003; McCollister, 2004; Singh and Ganju, 2004).

Many studies have found that large avalanche events are associated with particular weather events and upper atmospheric circulation patterns. For example, Hachler (1986) found that large avalanche events in the Swiss Alps are typically associated with quasi-stationary troughs that produce strong currents against the Alps and last approximately 4 days. In the Alps, avalanche activity was strongly associated with large storms, with west to northwest winds associated with avalanche activity in the Northern Alps, and southwest to southeast winds associated with avalanche activity in the Southern Alps (Hachler, 1986). Fitzharris (1987) found that all major avalanche winters in Canada were associated with a rapid switch in the mean monthly circulation during the middle of the winter season which created a weaker than normal zonal flow, followed by a return in the Westerlies causing large precipitation events to fall on a weakened snowpack. Previously Fitzharris (1981) determined that there are strong links between avalanche activity and atmospheric circulation, controlled by the 500mb pressure systems. Birkeland et al. (2001) determined that new snow and new snow water equivalent (SWE) were the most important factors in avalanche formation for their study areas, and that precipitation events creating large avalanche events were associated with very distinct 500mb circulation patterns. For example, large avalanche events in Taos, New Mexico (their study site closest to Gothic, Colorado) were most commonly associated with southwesterly flow suggesting these events are related to the maximum zone of upper-level divergence. These studies indicate that large avalanche cycles are

strongly associated with distinct weather patterns. Unlike the work here, these studies focus on large avalanche years instead of the avalanche system as a whole.

Rather than providing a specific model to be used for forecasting purposes in Gothic, Colorado, this study attempts to provide a quantitative statistical descriptive model describing of the effect daily precipitation and upper atmospheric wind direction and speed have on natural avalanche formation. In addition, this work also strives to provide a better understanding of why derived variables such as upper atmospheric wind direction and speed are relevant to backcountry avalanche forecasting. This will be done spatially by using maps to show the relationships and patterns of avalanche events in relation to the avalanche starting zone aspect and the direction of the 500mb wind. These study goals are best addressed by testing two simple hypothesizes: 1) Prevailing upper atmospheric winds are more likely to be associated with natural avalanches in avalanche paths with a starting zone aspect lee to the prevailing upper atmospheric free air winds, and 2) The odds of a natural avalanche occurring increases with increasing SWE, increasing upper atmospheric wind speeds, and depends on upper atmospheric wind direction.

METHODS

The first hypothesis in this study states that natural avalanches are more likely in avalanche paths with an aspect lee to the prevailing upper atmospheric free air wind direction. To test this I will compare the probability of an avalanche occurring in different groups of avalanche paths with similar starting zone aspects as well as individual starting zones to the upper atmospheric wind direction. The second hypothesis states that the odds of a natural avalanche occurring will increase with increasing upper atmospheric free air wind speeds as well as increasing new SWE and will be depend on upper atmospheric wind direction. A statistical model will be used to test this hypothesis.

There are two primary sources for the data used in this work. The avalanche data, avalanche path shapefiles and the new snowfall, new SWE, and temperature were all collected by billy barr and RMBL whereas the upper atmospheric wind data are from the National Centers for Environmental Prediction/National Centers for Atmospheric Research (NCEP/NCAR) Reanalysis Project. These data are discussed below.

Data

Avalanche Path and Avalanche Data

The avalanche paths surrounding Gothic, Colorado have been clearly defined by billy barr. Although billy barr attempts to collect information on every avalanche that occurs within the Gothic Valley, not all of the paths are equally visible from his observation points and therefore are not observed at the same frequency. They are divided into four groups; "always observed", "usually observed", "sometimes observed",

and "rarely observed" (Fig. 1). Only paths that fall into the classification of "always observed" and "usually observed" will be used in this analysis (Fig. 2, designated by starting zone). If avalanches that occurred in less frequently monitored avalanche paths were included in this study, the analysis would be skewed towards days with weather more convenient for monitoring conditions rather than a more even distribution of the entire study period as a whole.
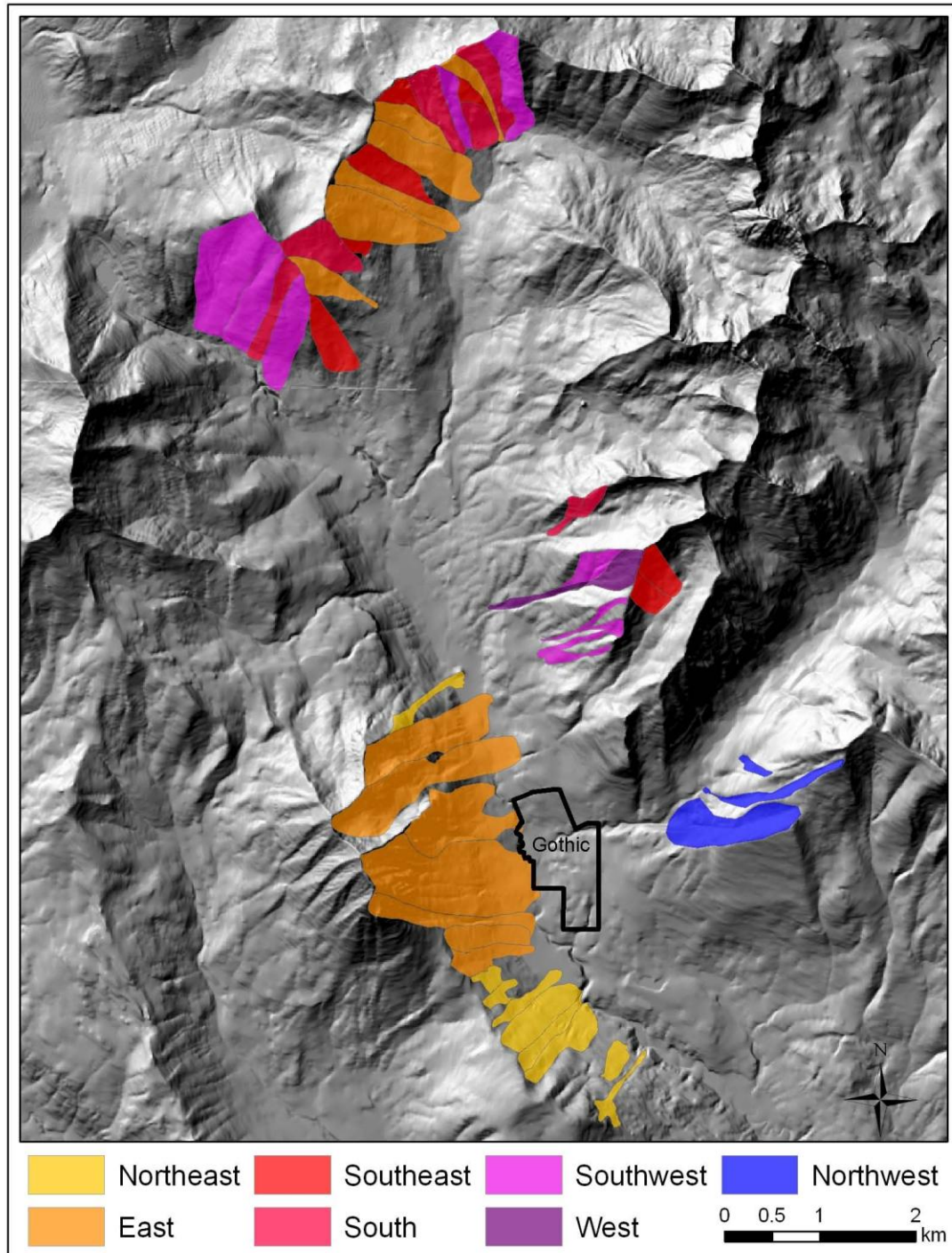
Figure 2: Always and frequently observed avalanche paths designated by their starting zone aspect (there are no paths with a north starting zone aspect in the Gothic Valley).

The avalanche data were collected according to the standard U.S. method (Perla and Martinelli, 1978, p. 225). However only three factors will be used in the first analysis: the day the avalanche occurred, the path the avalanche occurred in, and the avalanche type (only dry, slab avalanches are considered). This analysis attempts to test the effect upper atmospheric wind has on avalanche conditions at the valley-wide scale as well as in paths with a similar starting zone aspect and individual avalanche paths. The statistical model, on the other hand, will include the day the avalanche occurred, the avalanche type and avalanche size for all dry slab avalanches. Unlike the simple probability analysis, this method attempts to statistically describe the effect upper atmospheric wind direction and speed as well as new SWE all have on the avalanche hazard on the valley-wide scale as well as indicate if the odds of a natural avalanche increase or decrease with changing SWE, upper atmospheric wind direction, and upper atmospheric wind speed. This study is designed to be a descriptive model rather than a predictive model. A predictive model would only be applicable for predicting avalanches in the avalanche paths used in this study. A descriptive model, on the other hand will provide a better understanding of the processes affecting natural avalanche conditions within the Gothic Valley, as well as the estimated increases or decreases in avalanche hazard based on changing SWE, and upper atmospheric wind speed and direction.

Since the contributing factors for dry and wet snow avalanches vary considerably, the analysis presented here specifically addresses natural dry slab avalanches only. In addition, this study only addresses the winter months of December, January, February, and March. The dataset was incomplete for the earlier months in the season and April is

typically dominated by wet snow avalanches therefore is not representative of true "winter" conditions. The dataset was therefore reorganized to reflect these changes.

To test the first hypothesis, only avalanche days are considered, therefore a day with one small avalanche is considered to be the same as another day with many large avalanches. This study uses a basic method to compare avalanche days with avalanche starting zone aspect, based on the hypothesis that upper atmospheric wind direction influences natural avalanche activity. Therefore, a binary avalanche day/no avalanche day classification is sufficient. This binary system does not have as much of an effect on the analysis at the scale of individual paths, where it is rare to have multiple avalanches in a day. This analysis is designed to examine the relationship between upper atmospheric wind direction and avalanche events, regardless of the avalanche size.

In contrast, the statistical model considers size by using an avalanche hazard index similar to that used by Birkeland and Mock (2000). The avalanche hazard index is determined by squaring the size of the individual avalanches and then summing the squared sizes for each day. This methodology is better equipped to assess the daily avalanche hazard on the valley-wide scale. It considers the effect upper atmospheric wind has on avalanche size rather than a simple binary classification.

<u>Weather Data</u>

Gothic, Colorado is in a remote part of the state where very few weather stations exist. In addition to collecting avalanche data, billy barr also collects weather data, including new snowfall, new SWE, and high and low daily air temperature. These data are collected in the Gothic townsite on the valley floor. Although these data do not

provide precise weather measurements for each avalanche starting zone, they do reflect the overall weather trends within the valley.

There are no wind data collected within the Gothic Valley. Regardless, this study purposefully uses 500mb upper atmospheric wind data to assess the relationship between high-level wind and natural dry slab avalanche events for the winter months of December, January, February, and March. Previous work has indicated that terrain interactions may produce complex ridgetop winds. Therefore a specific ridgetop wind measurement may not always be the most useful for avalanche prediction over a large area (McCollister, 2004; Morrison, 2004). Upper atmospheric wind recordings for specific remote locations are difficult to obtain because it is difficult to get the required measurements, such as balloon soundings, at those locations. Therefore this work uses reanalyzed 500mb wind data from the NCEP/ NCAR Reanalysis Project (Kalnay et al., 1996). These data are output on a regular 2.5° latitude by 2.5° longitude grid with u and v in wind vector format at each point (the four closest locations to Gothic used in this work are shown in Fig. 3) where u represents the east-west vector and v represents the north-south vector. These data are determined with a dynamic data assimilation model that uses observed data from rawinsonde and pilot balloon data. Upper atmospheric wind data are in the most reliable class of reanalysis data ("A" type) and are therefore considered to be highly accurate because they are strongly influenced by actual observations. Details on the data collection and model details can be found in Kistler et al. (2001). These data are commonly used to establish upper atmospheric wind characteristics in specific areas (i.e. Perry et al., 2008; Myoung and Deng, 2009; O'Hara

et al., 2009; Bunya et al., 2010). Although this analysis follows standard methodology, it is important to remember that these data are reanalyzed and are therefore prone to inaccuracies such as local wind patterns and anomalies.
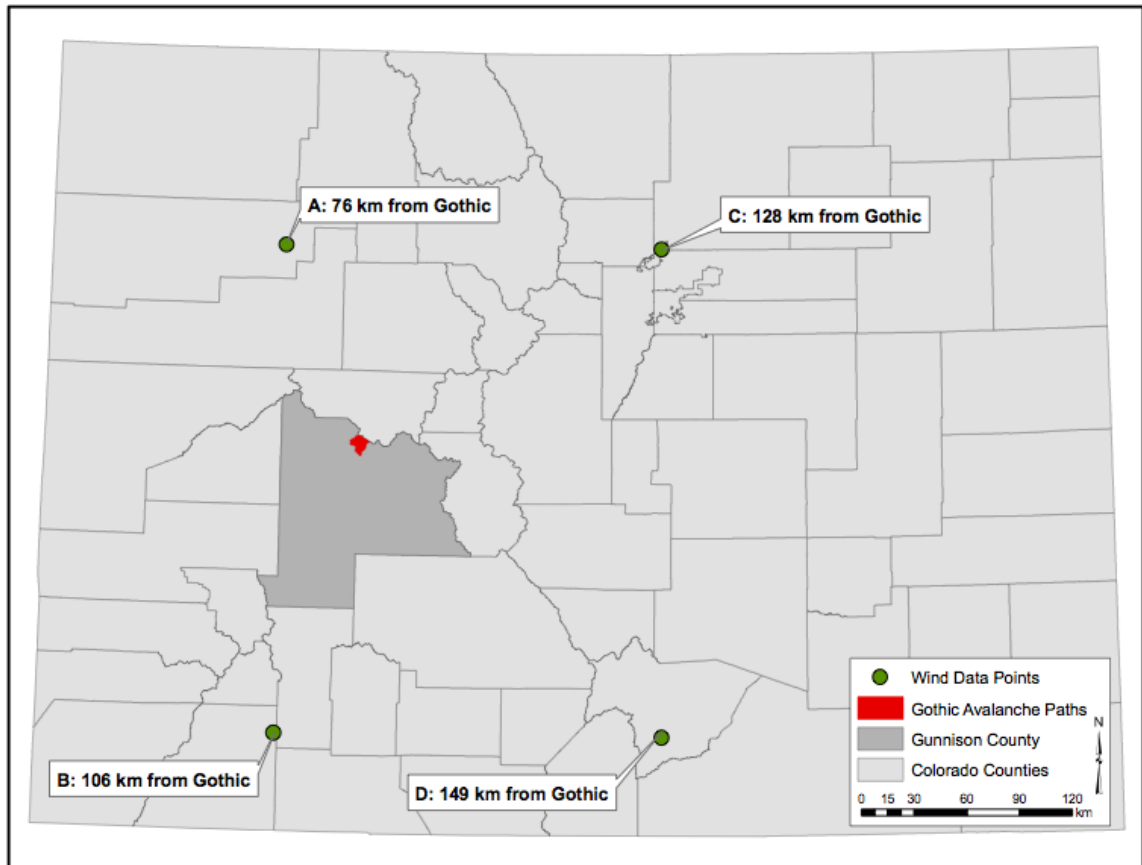
Figure 3: The four closest locations where NCEP upper atmospheric wind data are available.

The NCEP/NCAR reanalyzed upper atmospheric free-air-wind-vector data used in this work were collected at -107.5°, 40.0° (76 km from Gothic); -107.5°, 37.5° (106 km from Gothic); -105.0°, 40.0° (128 km from Gothic); and -105.0°, 37.5° (149 km from Gothic) (Fig. 3). Dr. Jacqueline J. Shinker obtained the raw u (east-west wind component) and v (north-south wind component) vector data used in this study. Once the

raw vector data was assembled and reduced to the study period of interest, an inverse

distance weighting (IDW) interpolation method (equation 1) was used to determine the

approximate daily upper atmospheric u and v wind vectors at Gothic, Colorado, where D_i

= the distance from known point to unknown point, P_i = value at known point, and W =

the unknown point. This calculation was done in a spreadsheet for each individual day in

the study period. IDW was chosen for its simple ability to interpolate from irregularly

spaced data to produce a continuous surface (Shepard, 1968).

$$(1) \qquad W = \frac{\sum_{i=1}^{n}(P_i(\frac{1}{D_i^2}))}{\sum_{i=1}^{n}(\frac{1}{D_i^2})}$$

Once this was complete, the u and v vectors were combined to determine both the 500mb

upper atmospheric wind direction (equation 2) and speed (equation 3) at Gothic for each

day during the study period using the following equations where u represents the east-

west wind component and v represents the north-south wind component.

$$(2) \qquad Direction = \arctan\left(\frac{-v}{-u}\right) \times \frac{180}{\pi} = 270 - \arctan\left(\frac{u}{v}\right) \times \frac{180}{\pi}$$

$$(3) \qquad Speed = \sqrt{u^2 + v^2}$$

This process also allows this study to test whether or not derived wind data can

accurately be used for avalanche forecasting purposes.

Obtaining Aspect and Slope for the Starting Zones

This study examines the avalanche dataset on three scales: the entire valley, paths

of similar starting-zone aspects (Fig. 2), and individual paths. In order to determine the

aspect for each avalanche starting-zone, avalanche path shapefiles as well as elevation

data for the Gothic Valley were collected. The avalanche paths used for this study were

digitized by billy barr with the help of the staff of RMBL. Ten-meter elevation data for

Gothic, CO were obtained from the USGS Seamless Web Server and were used to create

both a slope layer and an aspect layer for the area using Arc GIS 9.3.1. In order to

determine the starting-zone, track, and runout-zone, the slope raster layer was classified

into three groups: the area in the avalanche path with a slope greater than or equal to 30°

(starting zone), the area with a slope of less than 30° but greater than 10° (track), and the

area with a slope of less than or equal to 10° (runout zone). Using these groups each path

shapefile was divided into a starting-zone ($\geq$ 30°), track ($<$ 30° and $>$10°), and runout-

zone ($\leq$10°) by overlaying the avalanche path shapefile over the slope raster data and

manually editing the shapefiles by dividing them along the approximate boundaries

between the reclassified slope zones. The starting zones were exported into a new

shapefile and converted into a raster file.

Once the starting zone raster was created, the zonal statistics tool was used to

extract the mean, standard deviation, minimum, and maximum starting-zone aspect for

each avalanche path. Raw aspect data is difficult to work with due to the cyclic

(azimuthal) measurement scale. Therefore, aspect was reclassified into eight nominal

classes (Table 1). The reclassified aspect data and starting zone raster data were

combined using zonal statistics to extract the minimum, maximum, mean, standard

deviation, and the median aspect for each avalanche path starting zone. In order to

prevent the data from being skewed by outliers, the median was used to determine the

aspect for each starting zone.

Table 1: Direction Groups

Direction	Direction in Degrees
North (N)	337.5° – 22.5°
Northeast (NE)	22.5° – 67.5°
East (E)	67.5° – 112.5°
Southeast (SE)	112.5° – 157.5°
South (S)	157.5° – 202.5°
Southwest (SW)	202.5° – 247.5°
West (W)	247.5° – 292.5°
Northwest (NW)	292.5° – 337.5°

Analyzing Wind Direction

Both hypotheses tested with this analysis assess the effect upper atmospheric

wind direction has on avalanche conditions around the Gothic Valley. To test these

hypotheses two primary methods were used. The first uses methods similar to those of

McCollister (2004) and McCollister et al. (2003) where the probability of an avalanche

for starting zone aspect groups and individual paths is compared to the upper atmospheric

wind direction. The other uses the more robust two-component mixture model, also

known as a hurdle model (Greene, 1994; Welsh et al., 1996; Cameron and Trivedi, 1998; Dalrymple et al., 2002; Zeileis et al., 2008; Garrido et al., 2009; Walker et al., 2009). Hurdle models have been employed in ecological studies, but this study is the first application in avalanche sciences (Welsh et al., 1996; Garrido et al, 2009; Walker et al., 2009).

To prepare the data for basic upper atmospheric wind direction analysis for the valley-wide scale, aspect scale, and the individual path scale, the weather and avalanche databases were combined. To do this, the avalanche and weather databases were brought into and analyzed using ArcGIS 9.3.1. Using the query function the weather database was separated into eight groups based upon the average daily upper atmospheric wind direction (Table 1). The number of days in each wind group was then counted. Each group was related back to the avalanche data by counting the number of days in each wind group with an avalanche. The number of avalanche days in each wind group was divided by the total number of days in each wind group then multiplied by 100 to get the percent probability of an avalanche occurring with upper atmospheric wind from all eight directions. For example if there were 100 days when the dominant upper atmospheric wind was from the northwest, and 10 of those days were considered avalanche days, the probability of an avalanche occurring with a northwest wind would be 10/100 or 10%. This was done for all avalanche days on the valley-wide scale, the path aspect group scale and the individual path scale.

Statistical Model

Although log-linear regression for Poisson counts has traditionally been used to model rare count data (Ramsey and Shafer, 2002; Zeileis et al., 2008), it does not accommodate a large number of zeros. Avalanches are rare natural events that fall into this extreme zero category. In the winter seasons of 1975-1976 to 2007-2008 there were 3,892 days but only 775 avalanche days, indicating that approximately 80% of the days during the study period had no avalanche activity (Fig. 4). Two-component hurdle models are commonly used to correct for large numbers of zeros within datasets, especially in ecological and disease literature (Greene, 1994; Welsh et al., 1996; Dalrymple et al., 2002; Zeileis et al., 2008; Garrido et al., 2009; Walker et al., 2009). This type of model contains a hurdle component that models simply the zero and non-zero values and a log-linear Poisson component that models the positive counts (Cameron and Trivedi, 1998). This approach maximizes the estimates in a similar manner to many other regression models using maximum likelihood estimation (MLE). The difference is that there are two separate maximizations, one for the zeros, and the other for the counts greater than zero. The hurdle model also accounts for overdispersion (when the variance exceeds the mean) within the data by removing the zero counts from the Poisson model (Cameron and Trivedi, 1998). Both the binary and Poisson models use log-linear regression, therefore a back transformation from log space into arithmetic space will be needed for interpretation.

All days during the study period

Only days with an avalanche hazard of 1 or more
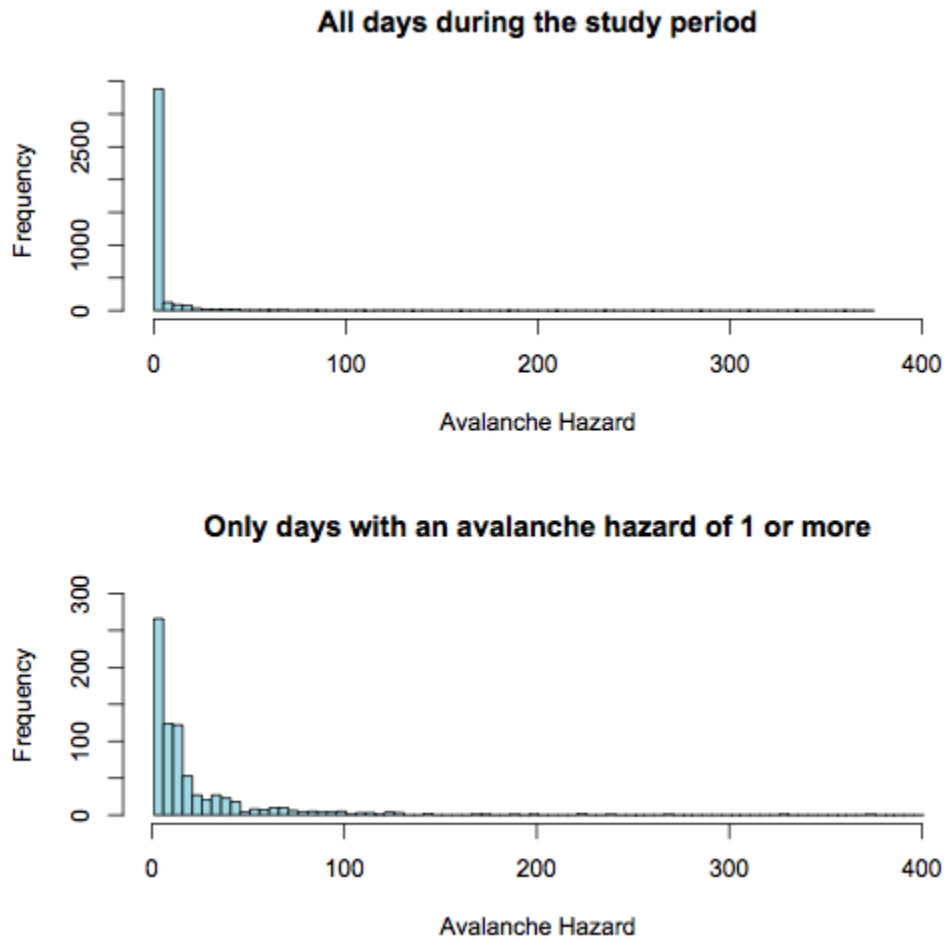
Figure 4: The top histogram shows the large number of zero avalanche hazard days during the study period. The bottom histogram shows only those days with a hazard of 1 or more.

An avalanche hazard index similar to that used in Birkeland and Mock (2001) was used as the response count value for the valley-wide hurdle model (Fig. 4). Rather than just accounting for the number of avalanches that occurred on each day, an avalanche hazard index also considers the relative size of the avalanche. To determine the daily avalanche hazard index, the sizes of the individual avalanches were squared and then summed for each day. Therefore a day with 4 class one avalanches and 2 class two

avalanches would have an avalanche hazard of 12 but a day with 4 class three avalanches and 2 class four avalanches would have a hazard of 68. If just the count of the daily avalanches was used, then both days would have a value of 6. This methodology therefore provides a better determination of the daily hazard as compared to just the daily count as it more accurately accounts for the larger, more dangerous avalanches, and subsequently provides a quantitative assessment of the effect upper atmospheric wind direction, upper atmospheric wind speed, and new SWE have on the actual avalanche danger level (according to the avalanche size) within the Gothic Valley.

This methodology attempts to define the effect wind has on natural avalanches within the Gothic Valley rather than the effect wind has on specific aspects. Therefore the hurdle method was only used for the valley-wide scale rather than the individual path scale or the starting zone aspect group scale. In addition to this, the valley wide scale is the only scale where the sample selection in each wind group is large enough for the results to be significant. There were simply not enough avalanches on the different starting zone aspects with upper atmospheric winds from each direction group for the model to be robust at a finer resolution than valley-wide.

The models were fit using new SWE, upper atmospheric wind speed, and upper atmospheric wind direction for each corresponding day. Wind direction is difficult to model because of its circular nature (Fisher, 1953). For an analysis such as this, a direction of 355° is essentially the same as 5°, therefore wind direction was divided into four groups reflecting north, east, south and west (Table 2). The eight wind direction groups used in the previous analysis were not used here because there were not enough

avalanche days in each wind group to allow assessment of significance within the

models. Whenever continuous data such as wind direction is put into groups, it ends up

being modeled as discrete data, meaning that each group is modeled with an individual

corresponding coefficient.

Table 2: Direction Groups for the statistical analysis

Direction	Direction in Degrees
North (N)	315° – 45°
East (E)	45° – 135°
South (S)	135° – 225°
West (W)	225° – 315°

The Multivariate Normal and t Distributions 0.9-9 package (mvtnorm) (Genz et

al., 2010), the Output analysis and diagnostics for Markov Chain Monte Carlo (MCMC)

Simulations 0.13-5 package (coda) (Plumer et al., 2010), and the hurdle function from

The Political Science Computational Laboratory, Stanford University 1.03 package (pscl)

(Jackman, 2010) in the R 2.9.2 system for statistical computing were all used for

modeling purposes in the work presented here. To determine the best-fit, the models

were compared using the Akaike's information criterion (AIC) which takes a measure of

the lack of fit of the model and then incorporates penalties for the number of terms in the

model (Ramsey and Schafer, 2002; Walker et al., 2009). The model with the lowest AIC

value will be used as the most appropriate model for these data.

RESULTS

Wind Direction Analysis

Valley-Wide Wind Direction Analysis

The dominant upper atmospheric wind direction in the Gothic Valley is west-northwest with very few wind days from the East (Fig. 5a). Therefore it is expected that the majority of the avalanches within the Gothic Valley will occur when the upper atmospheric winds are from west, northwest, and southwest simply due to the fact that those are the primary upper atmospheric wind directions (Fig. 5b). In order to better assess the effect that upper atmospheric wind direction has on natural avalanche conditions, the number of avalanche days in each wind direction group was normalized to the number of days the upper atmospheric wind blew from each direction. To do this I divided the number of avalanche days within each dominant upper atmospheric wind direction group by the number of days the upper atmospheric wind blew from the direction indicated by the group name (equation 4).

$$(4) \qquad \% P_i = \frac{A_i}{N_i} \times 100$$

Where P is the percent probability an avalanche will occur with wind from the different direction groups, i is the upper atmospheric wind direction group of interest, A is the

number of avalanche days with wind from the different direction groups, and N is the total number of days with wind from the different direction groups.

For example if there were 15 avalanche days out of the 30 days with upper atmospheric wind from the south the normalized avalanche probability for days with a southerly upper atmospheric wind would be 0.50 or 50%. This methodology allowed for a better comparison between the wind groups because it provides the likelihood or percent probability a day with upper atmospheric wind in each group would be considered an avalanche day (Fig. 5c). These data indicate that the valley is dominated by westerly upper atmospheric winds and the natural avalanches also tend to occur more often with westerly upper atmospheric winds (Fig. 5c). One interesting finding to note is the number of days with a northwesterly upper atmospheric flow are much greater than those with a southwesterly flow (Fig. 5a), yet the percent probability of an avalanche is much higher with upper atmospheric winds from the southwest (Fig. 5c).

Number of Days In Each Wind Group

Direction	Days
N	360
NE	69
E	27
SE	27
S	85
SW	631
W	1424
NW	1269

A

Number of Avalanche Days In Each Wind Group

Direction	Days
N	51
NE	5
E	2
SE	1
S	7
SW	139
W	368
NW	202

B

% Probability of an Avalanche Within The Gothic Valley With Different Upper Atmospheric Wind Directions

Direction	Probability
N	14.7
NE	7.3
E	7.4
SE	3.7
S	8.2
SW	22.0
W	25.8
NW	15.9

C

% Probability of Snow With Different Upper Atmospheric Wind Directions

Direction	Probability
N	29.7
NE	24.6
E	44.4
SE	37.0
S	55.3
SW	67.4
W	58.9
NW	38.7

D

Mean SWE (inches)

Direction	Mean SWE
N	0.18
NE	0.15
E	0.25
SE	0.14
S	0.30
SW	0.52
W	0.73
NW	0.29

E

Figure 5: Percent probability and count plots for different upper atmospheric wind directions at Gothic, Colorado. A) Number of days with average daily upper atmospheric wind direction from the different direction groups. B) Number of avalanche days associated with different upper atmospheric wind directions. C) Percent probability of a day being considered an avalanche day with different upper atmospheric wind directions. D) Percent probability of snow being associated with different upper atmospheric wind directions. E) Mean new snowfall expressed as SWE associated with upper atmospheric winds from each direction group.

The discovery that the number of days with a northwesterly upper atmospheric flow is much greater than those with a southwesterly flow prompted another hypothesis: Precipitation events are more commonly associated with southwesterly upper atmospheric flow. To test this hypothesis the number of days with precipitation from each upper atmospheric wind direction was divided by the number of days with upper atmospheric wind from each direction (Fig. 5d). These results indicate that southwesterly upper atmospheric flow is most commonly associated with winter precipitation events followed by westerly and then southerly upper atmospheric flow (Fig. 5d).

One interesting finding is that the percent probability of a day being considered an avalanche day with a southerly upper atmospheric wind is quite small relative to the avalanche percent probability with southwesterly and westerly upper atmospheric flow (Fig. 5c) especially since the percent probability of precipitation is approximately the same (Fig. 5d). To address this, the mean SWE associated with the eight upper atmospheric wind direction groups was calculated (Fig. 5e). The average SWE associated with westerly upper atmospheric flow is 0.73 inches whereas the SWE associated with southerly upper atmospheric flow is 0.30 inches (table in Fig. 5e). The SWE associate with southwesterly upper atmospheric flow is 0.51 inches (table in Fig. 5e). The results indicate that westerly events tend to be associated with more than twice the snow load of southerly events, and may partially explain why southwest winds are 1.4 times more likely to produce a natural avalanche within the Gothic Valley as compared to northwest winds. These results are similar to those presented for Taos, New Mexico in Birkeland et al. (2001). This will be further addressed in the discussion section.

West and southwest winds are most likely to produce an avalanche on the valley scale (Fig. 5c). Although this does make sense since those are the wind directions associated with larger precipitation events, remember that the methods used here do not differentiate between a day with one small avalanche and a day with several large avalanches. Any day with an avalanche is considered to be an avalanche day; therefore this analysis provides information regarding the relationship between upper atmospheric wind direction, precipitation, and natural avalanche events, not the daily avalanche hazard (such as avalanche size) associated with the upper atmospheric wind direction.

Ideally all of the results presented here for the different upper atmospheric wind groups would have equal importance, but this is not necessarily the case, especially for days with easterly upper atmospheric flow. There were only 27 days between the winter seasons of 1975-1976 and 2007-2008 when the dominant upper atmospheric wind was from both the east and the Southeast. The western United States is dominated by the westerly wind belts, therefore it is not surprising there were very few days when the dominant upper atmospheric wind direction was not from the west, northwest or southwest. Therefore, sample sizes for days with east and southeast upper atmospheric wind directions are not large enough to make any strong conclusions as to the effect of winds from the east and southeast. In addition, there were only 69 days with upper atmospheric winds from the northeast and 85 days with upper atmospheric winds from the south. Although the number of days in these groups is greater than the standard minimum statistical sampling size of 30, the sample size for the avalanche days in each of

those groups are all well below 10. Therefore all of these directions should be assessed

with caution. This will be addressed further in the following chapter.

Starting Zone Aspect Group and Path Scale Wind Direction Analysis

        Although it is helpful on the valley wide scale to understand the effect upper

atmospheric wind direction has on natural avalanches, it does not address the slope aspect

scale. To address the hypothesis that natural avalanches are more likely in avalanche

paths with a starting zone aspect lee to the prevailing upper atmospheric wind direction a

similar percent probability analysis was conducted on the seven path groups as well as on

each individual avalanche path within the Gothic Valley. For the slope aspect scale the

number of avalanche days that occurred with upper atmospheric winds from each

direction was divided by the number of days the upper atmospheric wind direction was

from the corresponding direction. The same was done for the individual path scale.

These data were mapped and plotted on the same image for comparison, and are

discussed individually below.

        The first four upper atmospheric wind groups have a sufficient number of

avalanche days for the analysis to be considered accurate, whereas the last four upper

atmospheric wind groups have such small corresponding avalanche days that these results

must be taken with caution. The sample sizes for the last four groups are too small for

any of the results to be significant.

North Upper Atmospheric Wind: When upper atmospheric winds are from the north,

avalanche starting-zones with a southerly aspect are expected to have the greatest

probability of a natural avalanche followed by paths with southeast or southwest starting-

zone aspects. There were 360 days with upper atmospheric winds from the north (N_i in

equation 4). East aspects have the greatest percent probability of having a natural

avalanche followed by south aspects (Table 3 and inset graph in Fig. 6). The individual

path with the greatest percent probability of a natural avalanche with north winds is

south-facing followed by another south-facing path (both are in the northern part of the

valley) and then an east-facing path (Fig. 6).

Table 3: Percent probability of an avalanche occurring in each starting zone aspect group
with upper atmospheric wind from the north.

Starting Zone Aspect	Avalanche Days (A_i)	Percent Probability
NE	6	1.7
E	33	9.2
SE	11	3.1
S	25	6.9
SW	9	2.5
W	1	0.3
NW	1	0.3

Figure 6: Map showing the percent probability of an avalanche in each path with upper atmospheric winds from the north. Inset map shows the percent probability of an avalanche for each avalanche path aspect group with winds from the north ($n = 360$) (the blue arrow represents the wind direction). See equation 4 for methodology.

<u>Northwest Upper Atmospheric Wind</u>: When upper atmospheric winds are from the northwest, avalanche starting zones with a southeasterly aspect are expected to have the greatest percent probability of having a natural avalanche followed by paths with south and east starting zone aspects. There were 1269 days during the study period with a dominant upper atmospheric wind direction from the northwest (N_i in equation 4). This is the second most dominant wind direction in the Gothic Valley (Fig. 5a). Path groups with an east facing starting zone have the greatest percent probability of producing an avalanche with a northwest upper atmospheric wind followed by northeast and then south facing starting zone aspect groups (Table 4 and Fig. 7). The individual path with the greatest percent probability of a natural avalanche occurring with a northwest upper atmospheric wind is located in the northern part of the valley and has a south facing aspect (Fig. 7).

Table 4: Percent probability of an avalanche occurring in each starting zone aspect group with upper atmospheric wind from the northwest.

Starting Zone Aspect	Avalanche Days (A_i)	Percent Probability
NE	51	3.5
E	128	10.1
SE	34	2.7
S	60	4.7
SW	33	2.6
W	2	0.2
NW	3	0.2

Figure 7: Map showing the percent probability of an avalanche in each path with upper atmospheric winds from the northwest. Inset map shows the percent probability of an avalanche for each avalanche path aspect group with winds from the northwest (*n* = 1269) (the blue arrow represents the wind direction). See equation 4 for methodology.

West Upper Atmospheric Wind: When upper atmospheric winds are from the west,

avalanche starting zones with an easterly aspect are expected to have the greatest percent

probability of having a natural avalanche followed by paths with southeast and northeast

starting zone aspects. There were 1424 days during the study period with a dominant

upper atmospheric wind direction from the west (N_i in equation 4). This is the most

dominant wind direction within the valley (Fig. 5a). Paths with an east aspect have the

greatest likelihood of having a natural avalanche with a dominant upper atmospheric

wind direction from the west followed by paths with a northeast and then a south facing

starting zone (Table 5 and Fig. 8). Many of the paths with a northeast aspect have a

strong chance of cross loading from the ridges above them with westerly upper

atmospheric flow (Fig. 8). The individual paths with the greatest percent probability of

having a natural avalanche occur with the dominant upper atmospheric wind direction

from the west are east facing (Fig. 8).

Table 5: Percent probability of an avalanche occurring in each starting zone aspect group
with upper atmospheric wind from the west.

Starting Zone Aspect	Avalanche Days (A_i)	Percent Probability
NE	156	11.0
E	310	21.8
SE	90	6.3
S	131	9.2
SW	88	6.2
W	12	0.8
NW	14	1.0

Figure 8: Map showing the percent probability of an avalanche in each path with upper atmospheric winds from the west. Inset map shows the percent probability of an avalanche for each avalanche path aspect group with winds from the west ($n = 1424$) (the blue arrow represents the wind direction). See equation 4 for methodology.

Southwest Upper Atmospheric Wind: When upper atmospheric winds are from the

southwest, avalanche starting zones with a northeasterly aspect are expected to have the

greatest percent probability of having a natural avalanche followed by paths with north

and east starting zone aspects. There were 631 days during the study period with the

dominant upper atmospheric wind direction from the southwest (N_i in equation 4). Paths

with an east facing starting zone have the greatest percent probability of having an

avalanche with southwest upper atmospheric winds followed by paths with a northeast

facing aspect (inset Fig. 9). The individual paths with the highest likelihood of a natural

avalanche with southwest upper atmospheric winds are east facing and are all on Gothic

Peak (Table 6 and Fig. 9).

Table 6: Percent probability of an avalanche occurring in each starting zone aspect group
with upper atmospheric wind from the southwest.

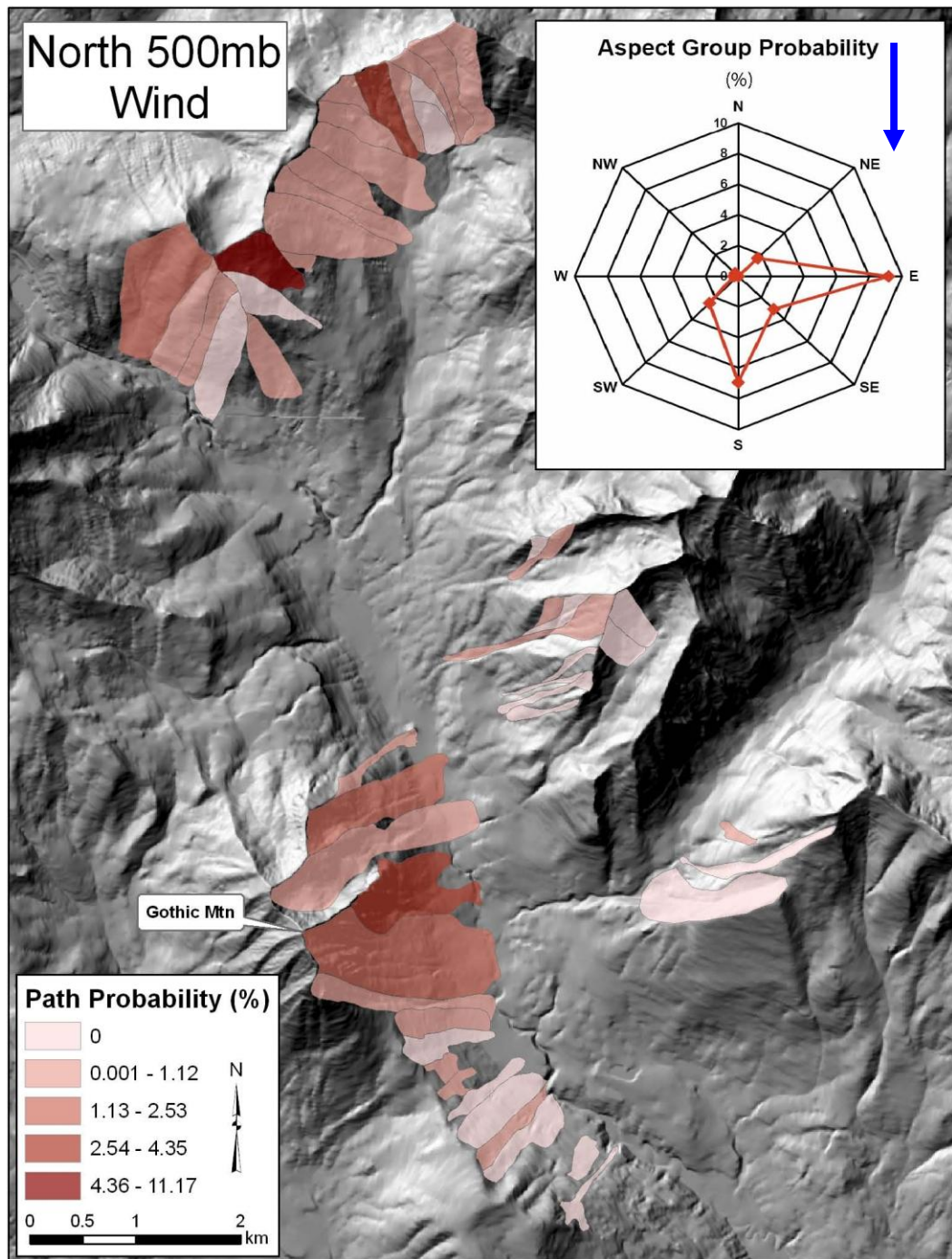| Starting Zone Aspect	Avalanche Days (A_i)	Percent Probability
NE	55	8.7
E	118	18.7
SE	27	4.3
S	35	5.6
SW	23	3.7
W	2	0.3
NW	6	1.0

Figure 9: Map showing the percent probability of an avalanche in each path with upper atmospheric winds from the southwest. Inset map shows the percent probability of an avalanche for each avalanche path aspect group with winds from the southwest ($n = 631$) (the blue arrow represents the wind direction). See equation 4 for methodology.

South Upper Atmospheric Wind: When upper atmospheric winds are from the south,

avalanche starting zones with a northerly aspect are expected to have the greatest percent

probability of having a natural avalanche followed by paths with northwest and northeast

starting zone aspects. There were 85 days with a dominant upper atmospheric wind

direction from the south (N_i in equation 4). Although it is expected that the paths with a

north starting zone aspect will have the greatest likelihood of having a natural avalanche

with a south upper atmospheric wind, there are no paths in the Gothic valley with a north

starting zone aspect (Fig. 3). South, southeast, and east path group aspects all have a

relatively higher percent probability (around 5%) of having an avalanche with upper

atmospheric winds from the south followed by paths with a southwest starting zone

aspect (Table 7 and Fig. 10). The individual path with the highest percent probability of

having an avalanche with southerly upper atmospheric winds also has a south facing

starting zone. Overall, there were also too few avalanche days with the upper

atmospheric wind from the south for these results to be very accurate (Table 7).

Table 7: Percent probability of an avalanche occurring in each starting zone aspect group
with upper atmospheric wind from the south.

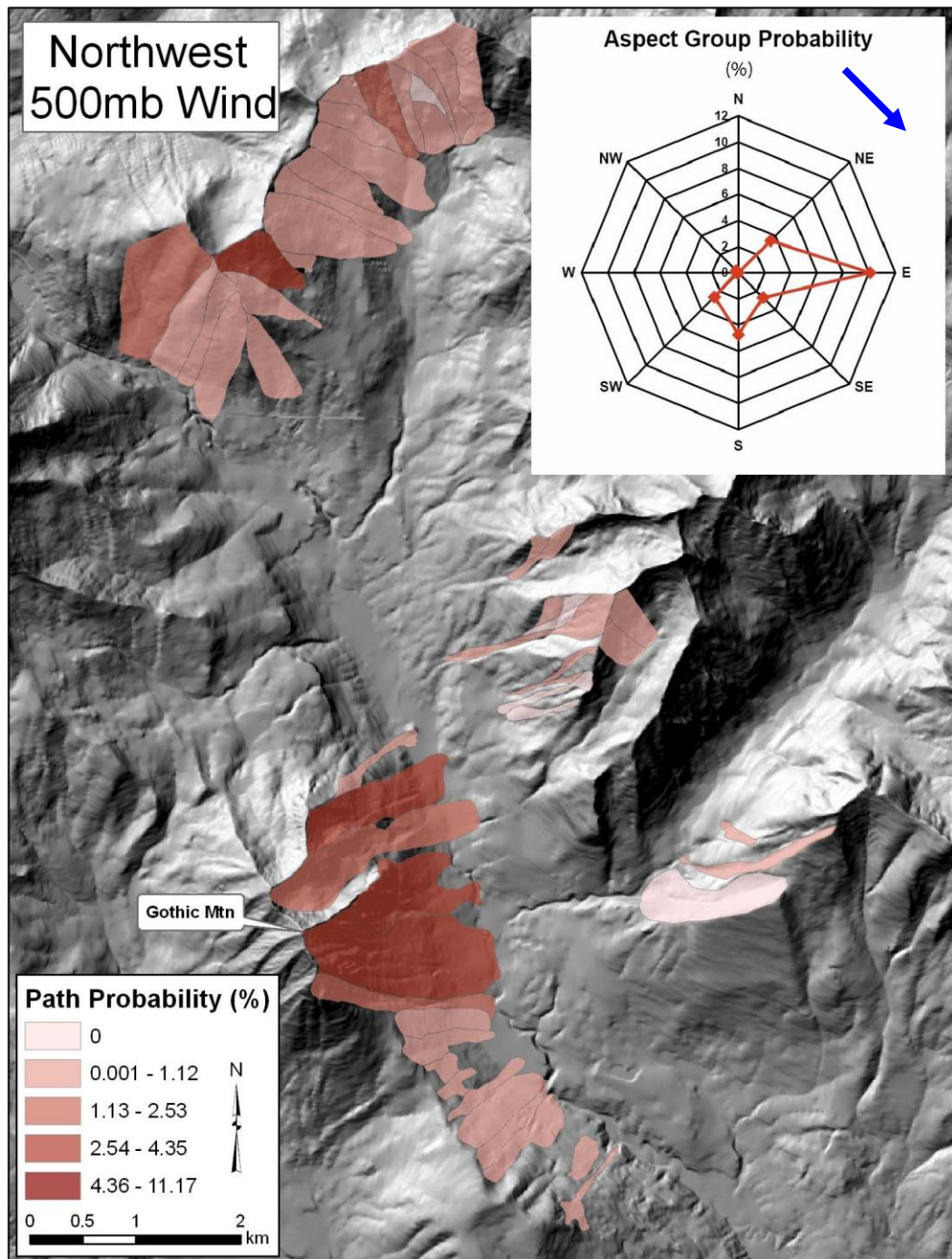| Starting Zone Aspect	Avalanche Days (A_i)	Percent Probability
NE	2	2.4
E	4	4.7
SE	4	4.7
S	4	4.7
SW	3	3.5
W	1	1.2
NW	1	1.2

Figure 10: Map showing the percent probability of an avalanche in each path with upper atmospheric winds from the south. Inset map shows the percent probability of an avalanche for each avalanche path aspect group with winds from the south ($n = 85$) (the blue arrow represents the wind direction). See equation 4 for methodology.

Southeast Upper Atmospheric Wind: When upper atmospheric winds are from the

southeast, avalanche starting zones with a northwesterly aspect are expected to have the

greatest percent probability of having a natural avalanche followed by paths with west

and north starting zone aspects. There were only 27 days during the study period with

upper atmospheric winds from the southeast (N_i in equation 4) therefore the results from

the southeast upper atmospheric wind analysis must also be interpreted cautiously (Fig.

11). There was only one avalanche on a day with dominant upper atmospheric wind

directions from the southeast and that was on a northeasterly aspect (Table 8 and Fig. 11).

Table 8: Percent probability of an avalanche occurring in each starting zone aspect group
with upper atmospheric wind from the southeast.

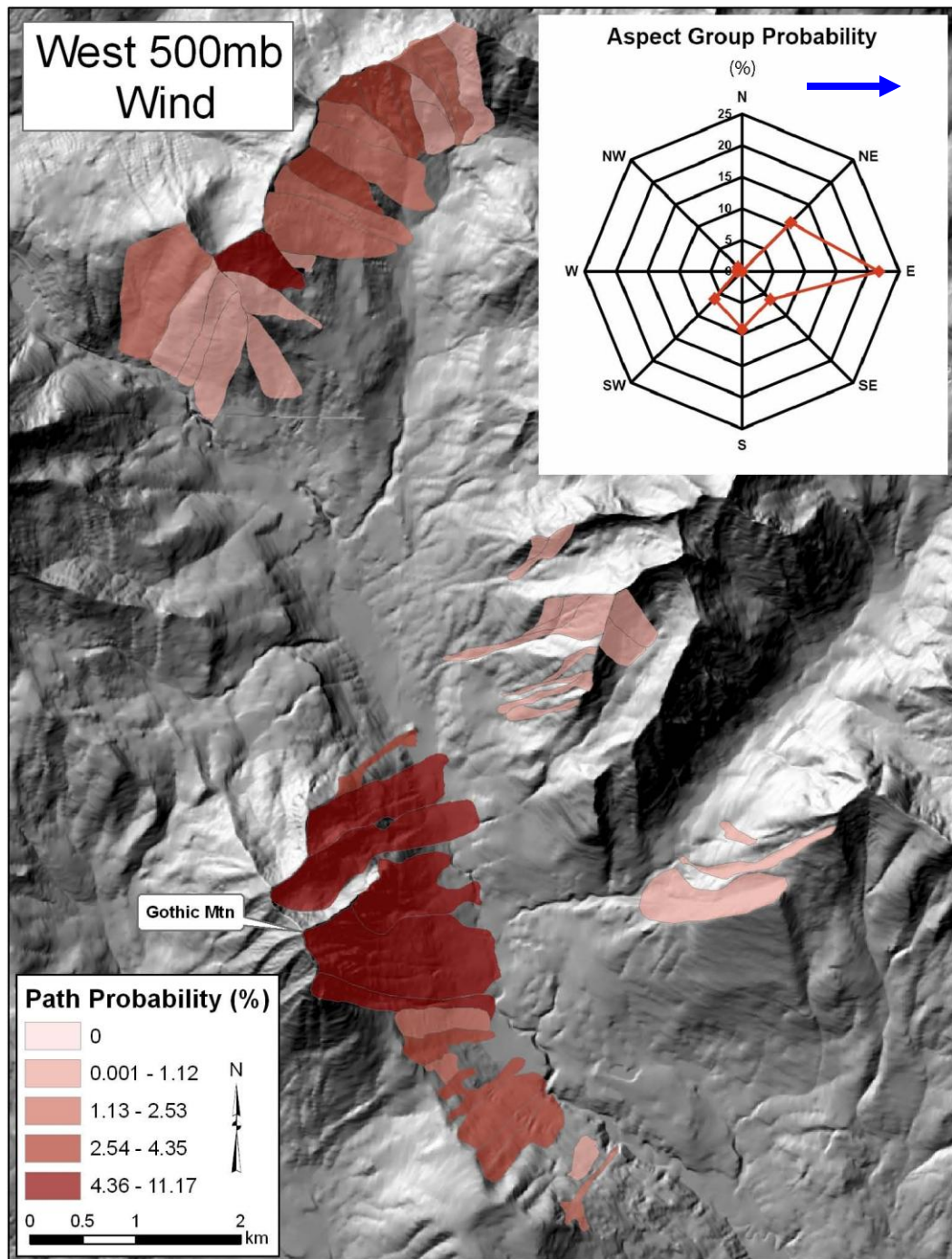| Starting Zone Aspect	Avalanche Days (A_i)	Percent Probability
NE	1	3.7
E	0	0.0
SE	0	0.0
S	0	0.0
SW	0	0.0
W	0	0.0
NW	0	0.0
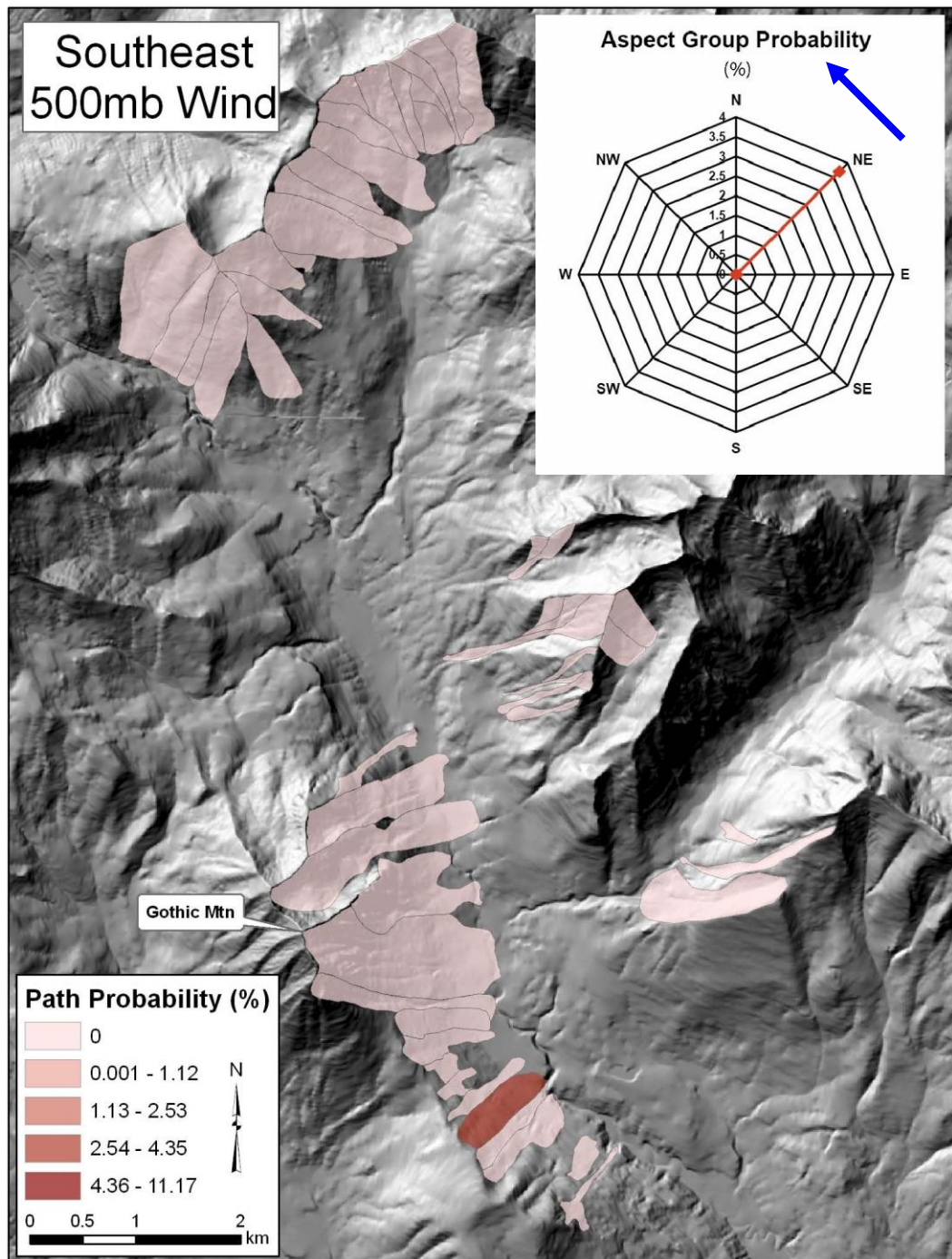
Figure 11: Map showing the percent probability of an avalanche in each path with upper atmospheric winds from the southeast. Inset map shows the percent probability of an avalanche for each avalanche path aspect group with winds from the southeast ($n = 27$) (the blue arrow represents the wind direction). See equation 4 for methodology.

East Upper Atmospheric Wind: When upper atmospheric winds are from the east, avalanche starting zones with a westerly aspect are expected to have the greatest percent probability of having a natural avalanche followed by paths with southwest and northwest starting zone aspects. There were only 27 days during the study period with a dominant upper atmospheric wind direction from the east (N_i in equation 4); therefore the results from the east upper atmospheric wind direction analysis must be interpreted with caution (Fig. 12). There were only two paths that had avalanches on days with dominant upper atmospheric wind direction from the east and there were only two natural avalanches within each of these paths (Table 9 and Fig. 12).

Table 9: Percent probability of an avalanche occurring in each starting zone aspect group with upper atmospheric wind from the east.

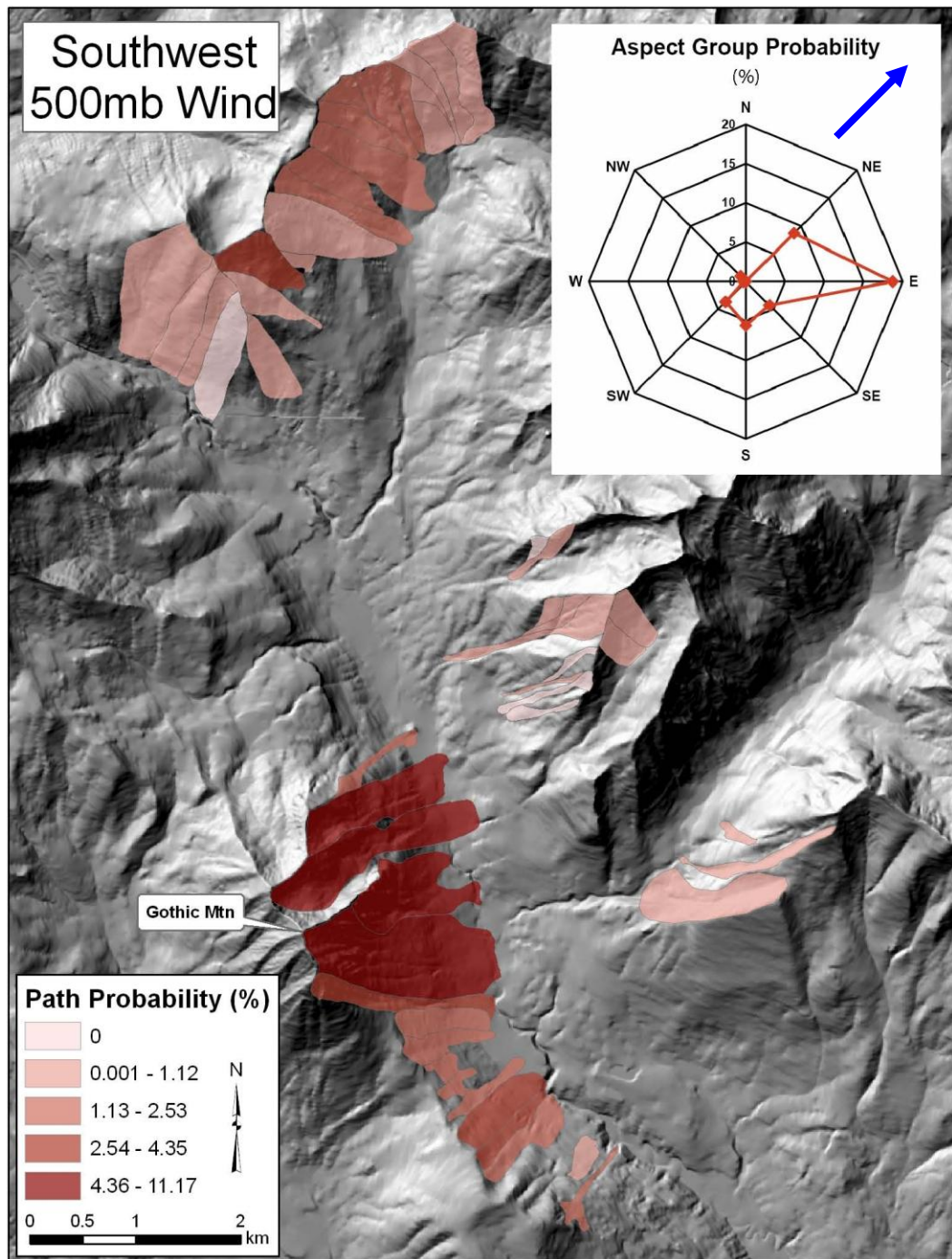| Starting Zone Aspect	Avalanche Days (A_i)	Percent Probability
NE	0	0.0
E	1	3.7
SE	0	0.0
S	0	0.0
SW	1	3.7
W	0	0.0
NW	0	0.0
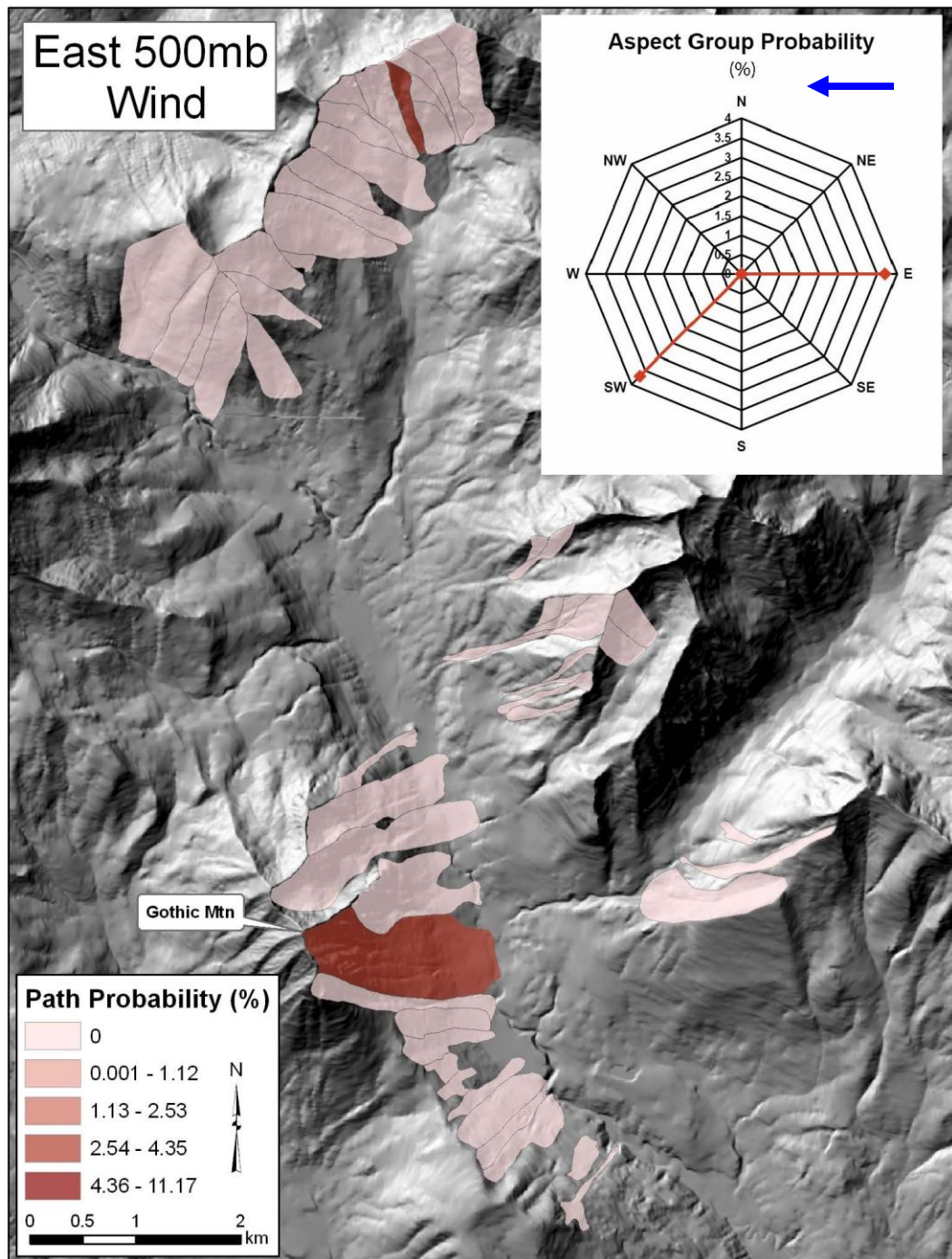
Figure 12: Map showing the percent probability of an avalanche in each path with upper atmospheric winds from the east. Inset map shows the percent probability of an avalanche for each avalanche path aspect group with winds from the east ($n = 27$) (the blue arrow represents the wind direction). See equation 4 for methodology.

Northeast Upper Atmospheric Wind: When upper atmospheric winds are from the

northeast, avalanche starting zones with a southwesterly aspect are expected to have the

greatest percent probability of having a natural avalanche followed by paths with south

and west starting zone aspects. There were 69 days during the study period with upper

atmospheric winds from the northeast (N_i in equation 4). The path group with the greatest

percent probability of a natural avalanche with an upper atmospheric northeast wind is

east facing, followed by southeast, southwest and finally south (Table 10 and inset graph

in Fig. 13). The individual paths with the highest percent probability of a natural

avalanche have an east facing starting zone (Fig. 13, Table 10).

Table 10: Percent probability of an avalanche occurring in each starting zone aspect group with upper atmospheric wind from the northeast.

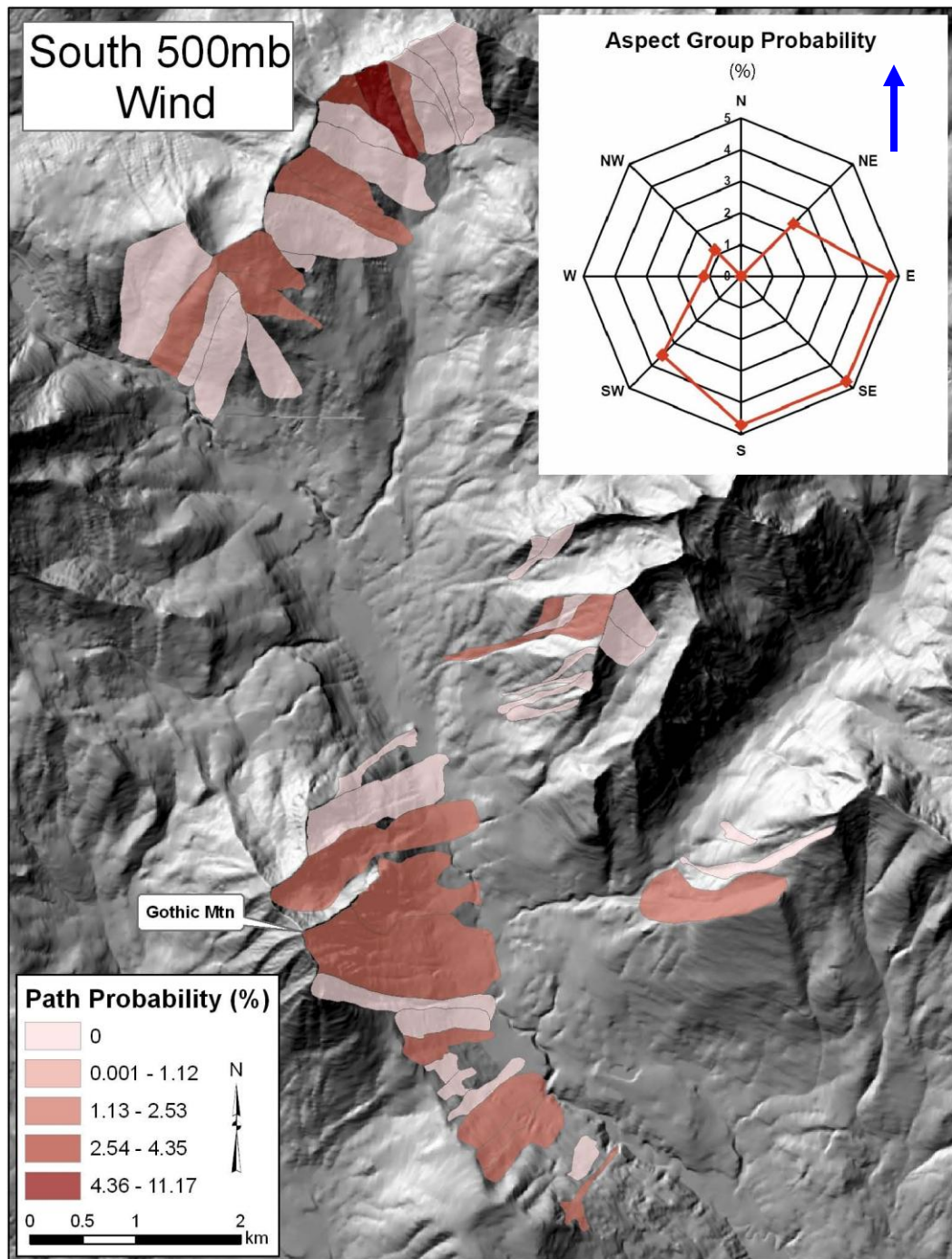| Starting Zone Aspect	Avalanche Days (A_i)	Percent Probability
NE	0	0.0
E	3	4.4
SE	2	2.9
S	1	1.5
SW	1	1.5
W	0	0.0
NW	0	0.0
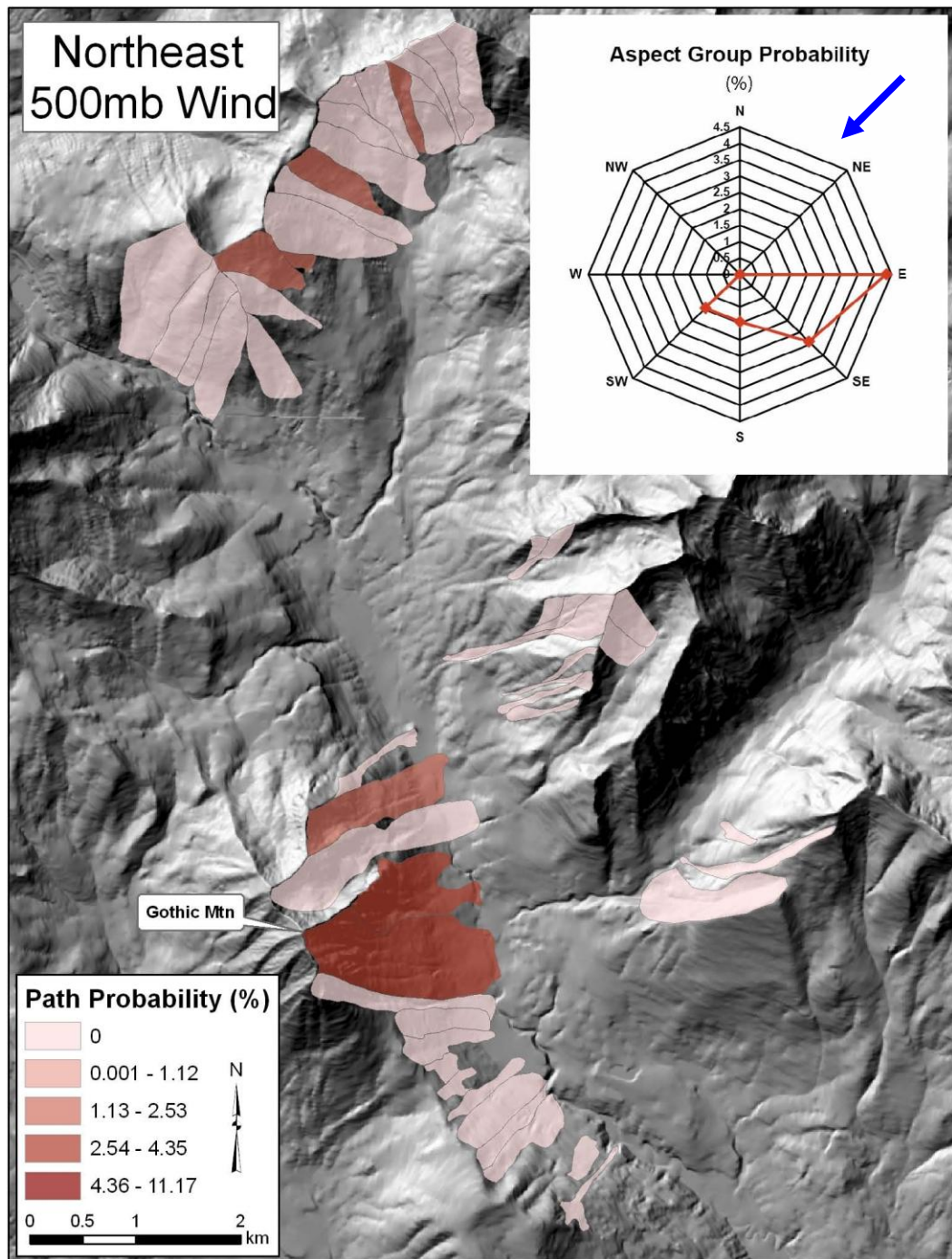
Figure 13: Map showing the percent probability of an avalanche in each path with upper atmospheric winds from the northeast. Inset map shows the percent probability of an avalanche for each avalanche path aspect group with winds from the northeast (the blue arrow represents the wind direction) (*n* = 69). See equation 4 for methodology.

Statistical Model

In order to determine the most appropriate hurdle model to use for this analysis, a hurdle model was first fit with new SWE, upper atmospheric wind speed and upper atmospheric wind direction, resulting in an AIC value of 23140 (Table 11). If a model with a variable removed has a lower AIC value than a model without a variable removed, then the variable should be removed (Ramsey and Schafer, 2002; Walker et al., 2009). When upper atmospheric wind direction was removed from the full hurdle model the more parsimonious model had a higher AIC value of 23255 (Table 11). This suggests that the full hurdle model is a better fit for these data. Next the full hurdle model was again reduced, this time keeping upper atmospheric wind direction and removing upper atmospheric wind speed. The AIC value from this assessment was 23160 (Table 11). Although this result was less than the AIC from the hurdle model containing SWE and 500mb wind direction, it did not produce a value less than that of the full hurdle model containing all of the regressors, indicating the full hurdle model is again a more appropriate fit for these data. In an attempt to reduce the AIC value from the full hurdle model, both upper atmospheric wind direction and speed were removed from the model, producing an AIC of 23278 (Table 11). Again this AIC value is higher than the full model, suggesting the full hurdle model is the most appropriate fit for these data. SWE was not removed from any of the models because the goal of the analysis was to determine the affect of upper atmospheric wind speed and upper atmospheric direction after accounting for new SWE. The previous analysis has indicated that the direction of upper atmospheric flow is important in determining the precipitation (Fig. 5d and e),

therefore this test was designed to test the effect of upper atmospheric flow after

accounting for precipitation.

Table 11: AIC values from the different model assessments. *Lowest AIC Value

Model	AIC Value
Full Hurdle Model	23140
Reduced Hurdle model with SWE and 500mb wind speed	23255
Reduced Hurdle Model with SWE and 500mb wind direction	23160
Reduced Hurdle Model with SWE	23278
Mixed Hurdle Model with different regressors for each component	23133*

Although the full model appeared to be the most appropriate model at this point,

not all of the variables were marked as significant. The model output suggested that

upper atmospheric wind direction was likely significant in explaining the variability for

the Poisson model, but not for the hurdle component, whereas upper atmospheric wind

speed was suggested to be significant for the hurdle component but not for the Poisson

model. This assessment led to the reduction of the hurdle component of the model by

removing upper atmospheric wind direction while retaining wind speed. In the Poisson

component, upper atmospheric wind speed was removed while upper atmospheric wind

direction was retained. This resulted in an AIC value of 23133, indicating that this was

the most appropriate model, as this model has the lowest AIC value. Therefore the

chosen model includes different sets of regressors for the hurdle component and the

Poisson component. This result indicates the Poisson model is conditional on the zero

hurdle model yet they are not dependent on the same variables (Zeileis et al., 2008). The

two models are stated in equations 5 and 6 (β_i refer to the regression coefficients or estimates).

(5)   Hurdle Component: $\text{Logit}(\pi) = \beta_0 + \beta_1\text{SWE} + \beta_2\text{speed}$ $\pi=0$

(6)   Poisson Component: $\text{Log}(\mu) = \beta_0 + \beta_1\text{SWE} + \beta_2\text{DIRECTION1} + \beta_3\text{DIRECTION2} + \beta_4\text{DIRECTION3}$ $\mu = 1,2,3\ldots$

There is convincing evidence that the odds of a day being considered an avalanche day increases as wind speed increases after accounting for new SWE (two-sided p-value <0.00001) (Table 12). After back transforming, it is estimated that there is a 38% greater chance of a day being considered an avalanche day with a 10m/s increase in the upper air wind speed, after accounting for new SWE, with a 95% confidence interval from 36% to 40% (Table 12).

There is convincing evidence that the mean daily avalanche hazard with a southerly upper atmospheric wind direction is greater than with a northerly upper atmospheric wind direction after accounting for SWE (two-sided p-value < .00001) (Table 12). After back transforming, it is estimated that the mean daily avalanche hazard when the upper atmospheric wind direction is from the south is 31% greater than when the upper atmospheric wind direction is from the north, with an approximate 95% confidence interval from 19% to 44% (Table 12).

Table 12: Parameter estimates, standard errors and p-values for the hurdle model. The binomial component models the odds of a day being considered an avalanche day after accounting for new SWE and the poisson model describes the daily avalanche hazard with a north wind compared to the other wind groups after accounting for new SWE.

	Model term	Estimate	Standard Error	p-value
Binomial Model	*constant* (β_0)	- 2.62	0.121	< 2e-16
	SWE (β_1)	+ 2.06	0.102	< 2e-16
	wind speed (β_2)	+ 0.03	0.006	< 2e-7
Poisson Model	*constant* (β_0)	+ 2.33	0.026	< 2e-16
	SWE (β_1)	+ 0.51	0.006	< 2e-16
	E wind direction (45˚-135˚) (β_2)	-0.59	0.203	< 4e-3
	S wind direction (135˚-225˚) (β_3)	+ 0.27	0.042	< 2e-10
	W wind direction (225˚-315˚) (β_4)	+ 0.28	0.029	< 2e-16

There is convincing evidence that the mean daily avalanche hazard with a westerly upper atmospheric wind direction is also greater than with a northerly upper atmospheric wind direction after accounting for SWE (two-sided p-value <.00001) (Table 12). After back transforming, it is estimated that the mean daily avalanche hazard when the upper atmospheric wind direction is from the west is 32% greater than when the upper atmospheric wind direction is from the west, with an approximate 95% confidence interval from 24% to 42% (Table 12).

There is convincing evidence that the mean daily avalanche hazard with a northerly upper atmospheric wind direction is greater than with an easterly upper atmospheric wind direction after accounting for SWE (two-sided p-value = 0.0038) (Table 13). After back transforming, it is estimated that the mean daily avalanche hazard when the upper atmospheric wind direction is from the north is 80% greater than when

the upper atmospheric wind direction is from the east, with an approximate 95%

confidence interval from 72% to 89% (Table 13).

Table 13: Parameter estimates, standard errors and p-values for the hurdle model. The binomial component models the odds of a day being considered an avalanche day after accounting for new SWE and the poisson model describes the daily avalanche hazard with an east wind compared to the other wind groups after accounting for new SWE.

	Model term	Estimate	Standard Error	p-value
Binomial Model	*constant* ($ß_0$)	- 2.62	0.121	< 2e-16
	SWE ($ß_1$)	+ 2.06	0.102	< 2e-16
	wind speed ($ß_2$)	+ 0.03	0.006	< 2e-7
Poisson Model	*constant* ($ß_0$)	+ 2.33	0.026	< 2e-16
	SWE ($ß_1$)	+ 0.51	0.006	< 2e-16
	N wind direction (45˚-135˚) ($ß_2$)	+ 0.59	0.203	< 4e-3
	S wind direction (135˚-225˚) ($ß_3$)	+ 0.85	0.204	< 3e-5
	W wind direction (225˚-315˚) ($ß_4$)	+ 0.87	0.202	<1.6e-5

There is convincing evidence that the mean daily avalanche hazard with a

southerly upper atmospheric wind direction is greater than with an easterly upper

atmospheric wind direction after accounting for SWE (two-sided p-value = .00003)

(Table 13). After back transforming, it is estimated that the mean daily avalanche hazard

when the upper atmospheric wind direction is from the south is 135% greater than when

the upper atmospheric wind direction is from the east, with an approximate 95%

confidence interval from 123% to 145% (Table 13).

There is convincing evidence that the mean daily avalanche hazard with a

westerly upper atmospheric wind direction is greater than with an easterly upper

atmospheric wind direction after accounting for SWE (two-sided p-value = .00002)

(Table 13). After back transforming, it is estimated that the mean daily avalanche hazard when the upper atmospheric wind direction is from the west is 139% greater than when the upper atmospheric wind direction is from the east, with an approximate 95% confidence interval from 128% to 150% (Table 13).

There is no evidence that the mean daily avalanche hazard with a westerly upper atmospheric wind direction is greater than with a southerly upper atmospheric wind direction after accounting for SWE (two-sided p-value = 0.62) (Table 14). After back transforming, it is estimated that the mean daily avalanche hazard when the upper atmospheric wind direction is from the west is 2% greater than when the upper atmospheric wind direction is from the south, with a 95% confidence interval from 1% to 3% (Table 14).

Table 14: Parameter estimates, standard errors and p-values for the hurdle model. The binomial component models the odds of a day being considered an avalanche day after accounting for new SWE and the Poisson model describes the daily avalanche hazard with a south wind compared to the other wind groups after accounting for new SWE.

	Model term	Estimate	Standard Error	p-value
Binomial Model	*constant* (β_0)	- 2.62	0.121	< 2e-16
	SWE (β_1)	+ 2.06	0.102	< 2e-16
	wind speed (β_2)	+ 0.03	0.006	< 2e-7
Poisson Model	*constant* (β_0)	+ 2.33	0.026	< 2e-16
	SWE (β_1)	+ 0.51	0.006	< 2e-16
	E wind direction (45°-135°) (β_2)	- 0.85	0.204	< 3e-5
	N wind direction (135°-225°) (β_3)	- 0.27	0.042	< 2e-10
	W wind direction (225°-315°) (β_4)	+ 0.016	0.034	0.62

DISCUSSION

Wind Direction Analysis

Valley-Wide Wind Direction Analysis

The dominant wind direction in the Gothic Valley is west, therefore it is not unusual to see the greatest number of avalanche days occur when the wind is from the west. There is, however a difference between the probabilities of a day being an avalanche day with upper atmospheric wind directions from the northwest (16%) compared to the southwest (22%) (Fig. 5c). According to a two-sample binomial test these probabilities are significantly different (p-value 0.001). This same test was conducted comparing the probabilities of a day being considered an avalanche day with upper atmospheric wind directions from each wind group. Southwest and west upper atmospheric wind groups are both significantly different from the other upper atmospheric groups more frequently than any other groups (Table 15). The only time southwest and west upper atmospheric wind groups are not significantly different from the other groups are when they are being compared to one another or when the probabilities for a southwest wind are compared to east winds. Remember there are too few days with upper atmospheric winds from any easterly directions for the two-sample binomial test to be accurate for the northeast, east, and southeast upper atmospheric wind direction groups. These results indicates that days with dominant upper atmospheric winds from the southwest and west are significantly more likely to produce an avalanche than days with dominant upper atmospheric winds from other directions.

Table 15: P-values from Two-sample binomial tests for equality of proportions comparing the probability of an avalanche with different upper atmospheric wind directions. Bold if significant (0.05 significance level).

		Upper Atmospheric Wind Direction							
		N	NE	E	SE	S	SW	W	NW
Starting Zone Aspect	N		0.171	0.487	0.213	0.200	**0.003**	**4.24E-06**	0.467
	NE	0.171		1.000	0.860	1.000	**0.006**	**0.001**	0.077
	E	0.487	1.000		1.000	1.000	0.116	**0.050**	0.350
	SE	0.213	0.860	1.000		0.713	**0.042**	**0.017**	0.144
	S	0.200	1.000	1.000	0.713		**0.005**	**4.32E-04**	0.081
	SW	**0.003**	**0.006**	0.116	**0.042**	**0.005**		0.073	**0.001**
	W	**4.24E-06**	**0.001**	**0.050**	**0.017**	**4.32E-04**	0.073		**4.19E-10**
	NW	0.467	0.077	0.350	0.144	0.081	**0.001**	**4.19E-10**	

The high percent probability of a day being considered an avalanche day with dominant upper atmospheric winds from the southwest as compared to the northwest is interesting since the dominant upper atmospheric wind is twice as likely to be from the northwest than from the southwest. This spurred the formulation of a post a priori hypothesis: precipitation is more likely when upper atmospheric winds are from the southwest than from the northwest. These precipitation-producing storms affiliated with southwest upper atmospheric flow are likely associated with mid-latitude cyclones where divergence is associated with low pressure and therefore likely to produce precipitation, and convergence is associated with high pressure and therefore clear skies (Fig. 14). The percent probability of a southwesterly flow being associated with precipitation is 67% compared to 39% with a northwesterly flow (Fig. 5d), and the mean SWE with a southwesterly flow is 0.52 inches compared to 0.29 inches with a northwesterly flow (Fig. 5e). These results do correspond to a possible explanation presented in Birkeland et al. (2001) and explained by Rossby waves in the upper atmosphere (Fig. 14).

The explanation provided in Birkeland et al. (2001) appears to be relevant for the

Gothic are as well, suggesting that the primary reason southwesterly and westerly upper

atmospheric flow produce more snow days is that upper air flow from the southwest and

west have fewer topographic barriers to overcome as compared to northwesterly upper air

flow (Perla and Martineli, 1976). When moisture laden air masses from the west and

southwest arrive at the mountains surrounding Gothic they still have enough available

moisture to produce precipitation with the orographic lift, whereas northwesterly upper

air masses have already had most of the available moisture removed from them due to the

orographic uplift from previous ranges. Orographic lifting is reported to be responsible

for 50% of winter precipitation in mountainous areas (McClung and Schaerer, 2006).

In addition to the topographical explanation, cyclonic uplift also potentially plays

a role in the different upper air wind directions being associated with precipitation and

therefore avalanche events. Although cyclonic uplift is reported to only be responsible

for 10% of winter precipitation in mountainous areas, it is still a factor that should be

addressed (McClung and Schaerer, 2006). Southwesterly flow is associated with

divergence in the upper atmosphere and therefore produces low pressure at the Earth's

surface (Fig. 14). This low pressure at the surface promotes cloudy or stormy weather,

which often produces precipitation (Aguado and Burt, 2001). In the northern hemisphere

convergence is associated with northwest winds and divergence is associated with

southwest winds (Fig. 14). The results are consistent with the conceptual model, which

predicts that precipitation events do lead to a larger avalanche hazard. This is likely a

contributing factor to the reason why the daily avalanche hazard is so much higher with

southwesterly upper atmospheric flow as compared to northwesterly upper atmospheric flow.
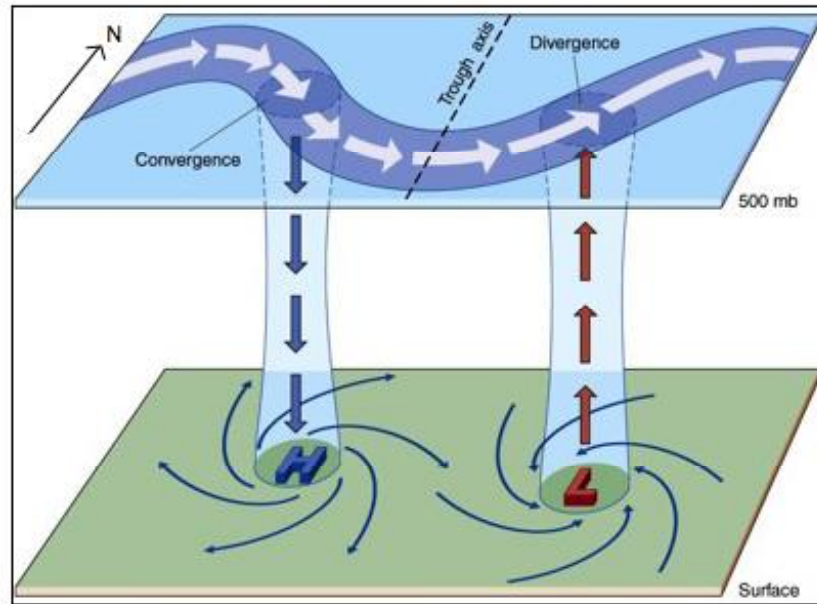
Figure 14: Rossby waves producing upper-level convergence and divergence creating high and low pressure on the Earth's surface (from Aguado and Burt, 2001, p. 269).

Although it would be ideal to have full confidence in this entire dataset, caution must be used when considering any winds from the east. There are such a small number of days with the wind from the east that the results from the easterly upper atmospheric flow analysis are likely skewed. There was only one day with an avalanche associated with an upper atmospheric wind from the southeast, two with the upper atmospheric wind from the east, five with the wind from the northeast and seven with the wind from the south, all of which are below a sample size of 30. It is also important to note that although weather data are commonly used for backcountry avalanche forecasting, it is not the only variable affecting avalanche formation. This study does not consider snowpack

layers or structure. Therefore there is inevitably some inherent error associated with the

analysis, and strong weight must not be applied to small sample sizes such as those with

an easterly upper atmospheric wind direction.

Starting Zone Aspect and Path Scale
Upper Atmospheric Wind Direction Analysis

The results from the slope and path scale analysis indicate that a relationship

might exist between upper atmospheric wind direction and starting zone aspect. Results

such as these suggest that upper atmospheric wind direction and starting zone aspect are

not independent and therefore do not follow the principle of parsimony (Crawley, 2007).

To test this hypothesis I used a Chi-squared contingency table (Table 16). The

hypothesis being tested is that the two variables are independent. Therefore if the

variables (upper atmospheric wind direction and starting zone aspect) are not independent

the null hypothesis will be rejected with a p-value less than 0.05 (Rogerson, 2006:

Crawley, 2007).

Table 16: Example of a 2x2 contingency table.

	Column 1	Column 2	Row totals
Row 1	a	b	$a + b$
Row 2	c	d	$c + d$
Column totals	$a + c$	$b + d$	n

The Chi-squared contingency tables use the observed frequency to determine the

expected frequency. The expected frequency assumes upper atmospheric wind direction

and starting zone aspect are independent and is calculated using equation 7, where E is

expected, R is the row total, C is the column total and G is the grand total (n from Table

6) (Rogerson, 2006: Crawley, 2007).

$$(7) \qquad E = \frac{R \times C}{G}$$

A Pearson's chi-squared test is then used to test for significant differences

between the observed and the expected frequencies. The observed frequencies are in

Table 16 and the observed probabilities are in Table 18. The observed avalanche

frequencies during the study period (Table 17) were compared to the expected

frequencies during the study period (Table 19) assuming upper atmospheric wind

direction and starting zone aspects are independent using Pearson's chi-squared test.

The test statistic is χ^2, the observed frequency is O, and the expected frequency is E

(equation 8) (Rogerson, 2006: Crawley, 2007).

$$(8) \qquad \chi^2 = \sum \frac{(O-E)^2}{E}$$

Table 17: Observed number of avalanche days during the study period for each starting zone aspect group with winds from the eight different upper atmospheric wind direction groups.*

		Upper Atmospheric Wind Direction							
		N	NE	E	SE	S	SW	W	NW
Starting Zone Aspect	NE	6	0	0	1	2	**55**	156	51
	E	33	3	1	0	4	118	**310**	128
	SE	11	2	0	0	4	27	90	**34**
	S	**25**	1	0	0	4	35	131	60
	SW	9	**1**	1	0	3	23	88	33
	W	1	0	**0**	0	1	2	12	2
	NW	1	0	0	**0**	1	6	14	3

Table 18: Percent Probability of an avalanche within each starting zone aspect group with different upper atmospheric wind directions.*

		Upper Atmospheric Wind Direction							
		N	NE	E	SE	S	SW	W	NW
Starting Zone Aspect	NE	1.7	0.0	0.0	3.7	2.4	**8.7**	11.0	3.5
	E	9.2	4.4	3.7	0.0	4.7	18.7	**21.8**	10.1
	SE	3.1	2.9	0.0	0.0	4.7	4.3	6.3	**2.7**
	S	**6.9**	1.5	0.0	0.0	4.7	5.6	9.2	4.7
	SW	2.5	**1.5**	3.7	0.0	3.5	3.7	6.2	2.6
	W	0.3	0.0	**0.0**	0.0	1.2	0.3	0.8	0.2
	NW	0.3	0.0	0.0	**0.0**	1.2	1.0	1.0	0.2

Table 19: Expected number of avalanches during the study period for each starting zone aspect group with winds from the eight different upper atmospheric wind direction groups assuming the variables are independent.*

		Upper Atmospheric Wind Direction							
		N	NE	E	SE	S	SW	W	NW
Starting Zone Aspect	NE	15.6	1.3	0.4	0.2	3.4	48.3	145.4	56.5
	E	34.4	2.8	0.8	0.4	7.6	106.4	320.3	124.4
	SE	9.7	0.8	0.2	0.1	2.1	29.9	90.1	35.0
	S	14.7	1.2	0.3	0.2	3.3	45.6	137.3	53.3
	SW	9.1	0.7	0.2	0.1	2.0	28.2	84.8	32.9
	W	1.0	0.1	0.0	0.0	0.2	3.2	9.7	3.7
	NW	1.4	0.1	0.0	0.0	0.3	4.5	13.4	5.2

*Bolded data are the starting zone aspects leeward of the 500mb wind direction.

The Pearson's chi-squared test indicates that the starting zone aspect and upper atmospheric wind direction are in fact independent of one another (p-value = 0.2998). This does appear to falsify the hypothesis that an avalanche is more likely to occur with an upper atmospheric prevailing wind lee to the starting zone aspect. The Pearson's chi-squared test is not necessarily the most appropriate test for these data, rather it is the only simple non-parametric contingency test that works with these data. When one or more of the expected frequencies is less than four then a Fisher's exact test is commonly used to test the contingency tables (Burt and Barber, 1996; Crawley, 2007). The expected frequency table (Table 19) indicates there are several expected frequencies less than four therefore Fisher's exact test should be used for these data. Although this would be ideal, it is not possible. The Fisher's exact test requires the factorial of the product of the row totals to be divided by the factorial of the individual frequencies to determine the percent probability of any one particular outcome (equation 9).

$$(9) \qquad p = \frac{(a+b)!(c+d)!(a+c)!(b+d)!}{a!b!c!d!n!} \qquad \text{values from Table 16.}$$

A desktop computer cannot complete this probability. Only a super computer could calculate the factorial of the row, column and grand total ($n=1493$) for this dataset. For this reason a Fisher's exact test cannot be used for analysis of these data with the tools available for this work.

Although Pearson's chi-squared test is not the most accurate contingency test, it is the best available for a dataset with large counts for several frequencies. Therefore, the

results from these contingency tables should be taken lightly. Although this is the case, comparisons can still be made for each starting zone aspect group.

In order to assist with this comparison, the wind direction lee to the starting zone aspect has been bolded in both Tables 17 and 18. Table 18 is more accurate for comparison as the values have been normalized for the number of days the upper atmospheric flow is from the corresponding direction. The hypothesis that prevailing upper atmospheric winds are more likely to be associated with natural avalanches in avalanche paths with a starting zone aspect lee to the prevailing upper atmospheric free air winds appears to only be directly true for east facing starting zones (Table 18). This work also attempts to consider cross loading so those wind directions close to the direction lee to the starting zone aspect are also analyzed. This does help to explain northeast and southeast starting zones (Table 18). Starting zones with a south facing aspect produce interesting results, as the highest percent probability for an avalanche to occur in an avalanche path in the south aspect group is with winds from the west, but the second highest is with winds from the north. This indicates that there could be other cross loading effects going on for certain paths within this aspect group. The only overriding results indicated by Table 18 are that westerly upper atmospheric winds produce the highest natural avalanche percent probability for all of the starting-zone aspect groups other than the west and the northwest starting zone aspect groups. This could possibly be due to the fact that west winds are associated with the highest mean SWE out of the eight wind direction groups (Fig. 5e). In order to better assess these results it appears that topography must also be taken into account (Fig. 6-13).

North Upper Atmospheric Wind: (Fig. 6, Table 3) North upper atmospheric winds are associated with a 9.2% probability of a natural avalanche occurring in an east facing starting zone. This is the highest likelihood out of the seven aspect groups with a north upper atmospheric wind (there are no paths with a north aspect therefore there are only seven starting zone groups). The second highest starting zone aspect group, with a 6.9% chance, are those paths with a south facing starting zone. The valley is dominated by east facing starting zones (13 paths with an east facing starting zone and only six with a south facing starting zone) therefore it is not surprising that the likelihood of having an avalanche is so much higher for east facing starting zones. Although there are more than twice as many paths with an east facing starting zone as compared to south facing, there is only a 30% greater likelihood of a natural avalanche occurring with northerly dominant upper atmospheric flow. Another explanation for the high overall probability for east aspects can be explained with cross loading. For example, the paths in the southern part of the valley surrounding Gothic Mountain appear to have a high potential for cross loading from the ridges to the north of the starting zone.

North upper atmospheric winds are associated with the highest avalanche probabilities (4.7% and 5.0%) in two separate south facing starting zones, and are both in the northern part of the valley (Fig. 2 for aspect). This is consistent with the hypothesis that northerly upper atmospheric winds are most likely to be associated with natural avalanches in paths with south starting zone aspects.

Northwest Upper Atmospheric Wind: (Fig. 7, Table 4) Northwest upper atmospheric winds are associated with a 10.1% probability of a natural avalanche occurring in an east

facing starting zone. This is the highest percent probability with a northeast upper

atmospheric wind out of the seven aspect groups. The hypothesis states that

northwesterly upper atmospheric flow will most commonly be associated with avalanches

in paths with a southeast starting zone aspect. Overall those paths with a southeast

starting zone aspect tend to have a lower frequency of avalanches in general (Table 17),

therefore it would be unrealistic to expect that the southeast group to have the highest

percent probability even with northwesterly upper atmospheric winds. Northwesterly

upper atmospheric winds are likely to cross load paths with an east aspect, especially

those paths on the southeast side of Gothic Mountain.

The individual path with the highest percent probability of having an avalanche

with northwesterly upper atmospheric flow is in the northern part of the valley and has a

south facing starting zone (Fig. 2 for aspect). This path does lie to the south of a ridge

running perpendicular to the northwest, therefore it is not surprising it has such a high

percent probability of producing a natural avalanche with northwesterly upper

atmospheric flow. The paths with the next highest probabilities are the east facing paths

off of Gothic Peak.

Overall these paths do appear to support the hypothesis that paths lee to the

dominant wind direction will tend to produce more avalanches than those windward to it.

The south-facing path in the northern part of the valley with the high percent probability

supports the hypothesis directly. The east facing paths on Gothic Peak support the

hypothesis after accounting for cross loading off of the ridges surrounding Gothic Peak.

West Upper Atmospheric Wind: (Fig. 8, Table 5) West upper atmospheric winds are associated with a 21.8% probability of a natural avalanche occurring in an east facing starting zone. This is the highest percent probability with a northeast upper atmospheric wind out of the seven aspect groups. Westerly upper atmospheric winds also produce the highest overall percent probability of having a natural avalanche on any aspect within the Gothic Valley.

When looking at the individual path percent probability, westerly upper atmospheric winds are associated with the highest percent probability of natural avalanches occurring in the Gothic Valley in the avalanche paths with an east facing starting zone in the southern part of the valley (Fig. 2 for aspect). Many of the paths in the northern part of the valley with larger percent probabilities appear to have a high chance of cross loading off of the ridges to the north of them. These results do indicate that the hypothesis is correct for westerly upper atmospheric winds.

Southwest Upper Atmospheric Wind: (Fig. 9, Table 6) Southwesterly upper atmospheric winds are associated with an 18.7% probability of a natural avalanche occurring in an east facing starting zone. The next highest percent probability of a natural avalanche occurring with a southwest upper atmospheric wind is 8.7% for starting zones with a northeast aspect. These results tend to support the hypothesis that southwesterly upper atmospheric flow is most likely to be associated with natural avalanches in paths with northeast and east starting zones.

All of the paths with a large percent probability (darkest color) surrounding the city of Gothic appear to be situated well to accumulate wind deposited snow with

southwesterly wind. This southwesterly upper atmospheric wind could remove the snow off of the southwest side of Gothic Mountain and deposit it on the east aspects because of the bowl shaped starting zones. It should also be noted that southwesterly and westerly upper atmospheric flow are also commonly associated with avalanches in those paths to the south of Gothic (Fig. 9 and 8).   These paths have relatively low angle starting zones therefore they do not tend to avalanche as frequently as those paths to the north of them with steeper starting zones.

Overall these results do support the hypothesis that southwesterly upper atmospheric flow will most commonly be associated with natural avalanches in paths with northeast (as well as east) starting zone aspects.

South Upper Atmospheric Wind: (Fig. 10, Table 7) South upper atmospheric winds are associated with a 4.7% probability of a natural avalanche occurring in an east, southeast, and south facing starting zone. This is somewhat counterintuitive when considering the hypothesis that southerly upper atmospheric wind are most likely to be associated with natural avalanches in paths with north facing starting zones, but there are no paths within the Gothic Valley with a north facing starting zone. Therefore the hypothesis cannot be accurately tested. It could then be argued that without any starting zones with a north aspect northeast and northwest aspects should have the highest percent probability of a natural avalanche, but these results do not indicate this to be the case.

The individual avalanche paths do not always follow the hypothesis that south winds are most likely to be associated with avalanches in paths with northeast and northwest starting zone aspects. The path most commonly associated with southerly

upper atmospheric wind is also south facing (Fig. 2 for aspect). This indicates the possibility of cross loading off of the ridge to the west of it with southerly upper atmospheric flow. The path to the north of Gothic Mountain, located in the large cirque could also be cross loaded with southerly upper atmospheric flow therefore the hypothesis is not completely rejected but it is not also completely supported.

There were only 85 days out of the 3892 days within the study period when the dominant upper atmospheric wind direction from the south. In addition to this, the sample size for the avalanche days with each wind direction are all too small to be accurately tested. Therefore these results must also be interpreted with caution.

Southeast Upper Atmospheric Wind: (Fig. 11, Table 8) There were only 27 days out of the 3892 days in the study period where the dominant upper atmospheric flow was from the southeast. Within those 27 days there was only one avalanche. Therefore these results provide inconclusive evidence for any relationship between upper atmospheric wind direction and starting zone aspect.

East Upper Atmospheric Wind: (Fig. 12, Table 9) There were only 27 days out of the 3892 days in the study period that where the dominant upper atmospheric flow was from the east. Although the results from the individual path analysis indicate a relatively high percent probability of 7% for an avalanche associated with east upper atmospheric wind, this is likely a false assessment due to the extremely small number of days with an east upper atmospheric wind. Within those 27 days there were two separate avalanches. The sample size is simply not large enough for a robust probability analysis to be conducted.

Therefore these results provide inconclusive evidence for any relationship between upper atmospheric wind direction and starting zone aspect.

Northeast Upper Atmospheric Wind: (Fig. 13, Table 10) Northeast upper atmospheric winds are associated with a 4.4% probability of a natural avalanche occurring in an east facing starting zone. This is the highest percent probability with a northeast upper atmospheric wind out of the seven aspect groups. The second highest percent probability is 2.9% for the southeast starting zone aspect group. These results are not consistent with the hypothesis that northeasterly upper atmospheric winds are most likely to be associated with natural avalanches in paths with southwest starting zone aspects. In fact, only one path with a southwest starting zone aspect had an avalanche occur on a day with northeast upper atmospheric winds (the red path furthest to the north) (Fig. 2 for aspect).

Although these results appear to contradict the original hypothesis, this contradiction should also be interpreted with caution. There were only 69 days out of the 3892 days in the study period that were dominated by northeasterly upper atmospheric flow. In addition, the number of avalanche days associated with the different wind groups are also very low (with the highest value being 3), therefore similar to the three previous groups, these results provide inconclusive evidence for any relationship between northeast upper atmospheric wind direction and starting zone aspect.

These avalanches that did occur could have also been caused by other factors affecting avalanche formation such as snowpack structure. Although these results generally negate the hypothesis, many of the individual paths could be cross-loaded with northeasterly upper atmospheric flow. For example the two large paths on the east side

of Gothic Peak have a relatively high likelihood of a natural avalanche. Northeasterly upper atmospheric flow could be redistributing snow from the north side of the ridge onto the south side into those two starting zones; therefore the hypothesis is not completely rejected.

<u>Statistical Model</u>

The results from the binomial component of the hurdle model indicate that after accounting for new SWE, upper atmospheric wind speed can be used to help determine if a day will be considered an avalanche day or not (Equations 3 and 4, Tables 12, 13, and 14). This shows that as the wind speed increases the hazard of an avalanche occurring somewhere within the Gothic Valley increases. As the wind speed increases, more snow is transported to starting zones, therefore increasing the odds of an avalanche. These results demonstrate that if there was a set amount of new SWE two different days, but the upper atmospheric wind speed for one day was 5m/s and the other was 15m/s the daily avalanche hazard would increase by 38%. Therefore if the hazard for the 5m/s day was 15 the hazard for the 15m/s day would be 20.7.

The results from the Poisson component of the hurdle model indicate that once a day is determined to be an avalanche day and after new SWE is accounted for, the avalanche hazard will be highest with southerly and westerly upper atmospheric winds (Table 12 and 14) followed by northerly upper atmospheric winds (Table 13) and finally lowest with easterly upper atmospheric winds (Table 13) (refer to written results section). This implies that for four days all with the same new SWE, the avalanche hazard will be the highest with a west or south upper atmospheric wind and lowest with an east upper

atmospheric wind. This also indicates that the avalanche hazard after accounting for new

SWE is essentially the same with a south upper atmospheric wind as it is for a west upper

atmospheric wind. These results are consistent with the previous valley-wide analysis

where days with the highest percent probability of producing an avalanche have west and

southwest upper atmospheric flow.

CONCLUSIONS AND FUTURE WORK

<u>Conclusions</u>

The results from this analysis show the usefulness of derived upper atmospheric wind direction for avalanche forecasting. Upper atmospheric wind direction does not completely explain avalanche events in Gothic, Colorado. However, 500mb wind does appear to be an important factor in determining the percent probability of an avalanche occurring as well as the daily avalanche hazard. After visually accounting for possible cross loading from interactions with the surrounding ridges it does appear that prevailing upper atmospheric winds are most likely to be associated with natural avalanches in avalanche paths with a starting zone lee to the prevailing upper atmospheric free air wind.

These results are important for remote backcountry avalanche forecasting because reliable ridge top data are rarely available and it is not always practical for the forecaster to make physical observations on a daily basis. This work will hopefully provide the backcountry avalanche forecaster with more confidence in using derived wind data for their regional forecasts of general avalanche conditions with respect to aspect. In addition, this also provides more evidence as to why such daily avalanche forecasts should not be mapped for the general public. On the valley wide scale upper atmospheric wind direction can be helpful for determining the overall avalanche danger, but as can be seen from the slope specific analysis variation does exist. Not all of the paths follow the general principal that upper atmospheric winds lee to the starting zone aspects will be associated with more avalanche activity. There are other contributing factors such as

cross-loading and snowpack structure. Thus, mapping regional forecasts onto specific slopes is an example of inappropriate downscaling of information. Regional forecasts have proven to be highly useful for the public, but downscaling that regional information to the path scale through mapping could be dangerous.

The work presented here also indicates how important basic physical processes such as orographic uplift and Rossby waves in the upper atmosphere are in shaping the daily avalanche hazard. There are fewer terrain barriers to the west and the southwest of Gothic to lift, cool, and dry air masses. Therefore there is more available moisture in air masses with a west or a southwesterly flow. In addition to this, but likely not to the same magnitude, southwesterly flow tends to create divergence in the upper atmosphere causing low pressure at the surface. This low pressure mixed with orographic lifting causes snowfall producing winter storms. The avalanche patterns within Gothic Valley follow this pattern quite well. There are many other factors involved in natural avalanche formation such as weak layers within the snowpack, but this work emphasizes the importance of variables as basic as upper atmospheric wind and new SWE.

New SWE is the most important weather variable for avalanche prediction in Gothic, Colorado, a finding consistent with other avalanche and weather studies (Buser et al., 1985; McCollister et al., 2003). After accounting for new SWE, wind speed is significant in determining whether or not an avalanche will occur within the Gothic Valley. This provides evidence that increased wind speed transports more snow and therefore increases avalanche activity. After the initial hurdle of determining a day to be an avalanche day or not is crossed, this work has determined that after accounting for

new SWE, wind direction is a significant variable when determining the overall avalanche hazard for the day, likely due to interactions between the wind and the surrounding topography.

Future Work

As with any database as large as the one from Gothic, Colorado, there are many more questions that could be tested with these data. For example, a similar study to the one presented here could be done for wet snow avalanches as well as loose snow avalanches, as this work only accounts for dry slab avalanches. It would be interesting to see if new snow and upper atmospheric wind can account for as many of the wet snow avalanches or if another variable such as temperature should be included in the analysis. Wet snow avalanches are typically associated with increasing temperatures above freezing, since liquid water needs to exist in the snowpack for a wet snow avalanche to occur. This suggests that temperature above and temperature below freezing level as well as the overall energy balance would be important to include in a similar analysis for wet snow avalanches. Therefore I would expect different weather variables, particularly temperature and solar radiation, would be needed to predict wet snow avalanches in the Gothic Valley. Loose snow avalanches, on the other hand are typically attributed to new snow therefore I would expect SWE to be the most important factor for a similar analysis on loose snow avalanches.

It would also be interesting to explore the exact weather conditions leading up to the largest avalanche cycles in the Gothic Valley. This could be done by conducting a

detailed analysis on the weather during and directly before the avalanche cycle, as well as considering the weather patterns and cycles throughout the winter season leading up to the event. This could be done in a way similar to methods presented by Fitzharris (1981 and 1987), Hachler (1986), and Birkeland et al. (2001). An analysis of this type would provide a better understanding of the weather events occurring several days, weeks, or even months before large avalanche events.

REFERENCES

Armstrong, R.L., and Armstrong, B.R., 1987, Snow and avalanche climates of the western United States: International Association of Hydrological Sciences Publications, v. 162, p. 281-294.

Aguado, E., and Burt, J.E., 2001, Understanding Weather and Climate – Second Edition: Upper Saddle River, New Jersey, Prentice-Hall, Inc., 505 p.

Bakkehøi, S., 1986, Snow avalanche prediction using a probabilistic method, *in* Proceedings of the Davos Symposium, Davos, Switzerland, p. 549-555.

Birkeland, K.W., Mock, C.J., and Shinker, J.J., 2001, Avalanche extremes and atmospheric circulation patterns: Annals of Glaciology, v. 32, p. 135-140.

Brabec, B. and Meister, R., 2001, A nearest-neighbor model for regional avalanche forecasting: Annals of Glaciology, v. 32, p. 130-134.

Bunya, S., Dietrich, J.C., Westerink, J.J., Westerink, H.J., Ebersole, B.A., Smith, J.M., Jensen, R., Resio, E.T., Atkinson, J.H., Roberts, H.J., Luettich, R.A., Dawson, C., Cardone, V.J., Cox, A.T., and Powell, M.D., 2010, A high-resolution coupled riverine flow, tide, wind, wind wave, and storm surge model for Southern Louisiana and Mississippi. Part I: Model development and validation: Monthly Weather Review, v. 138, p. 345-377.

Burt, J.E. and Barber, G.M., 1996, Elementary statistics for geographers, second edition: New York, New York, The Gilford Press, 640p.

Buser, O., 1983, Avalanche forecast with the method of nearest neighbours; an interactive approach: Cold Regions Science and Technology, v. 8, p. 155-163.

Buser, O., Fohn, P., Good, W., Gubler, H., and Salm, B., 1985, Different methods for the assessment of avalanche danger: Cold Regions Science and Technology, v. 10, p. 199-218.

Buser, O., 1989, Two years experience of operational avalanche forecasting using the nearest neighbours method: Annals of Glaciology, v. 13, p. 31-34

Cameron, A.C. and Trivedi, P.K., 1998, Regression Analysis of Count Data: New York, Cambridge University Press, 432 p.

Campbell, C., Jamieson, B., and Hageli, P., 2004, Small-scale mapping of snow stability: If not, why not: Avalanche News, v. 71, p. 45-49.

Crawley, M.J., 2007, The R book: West Sussex, England, John Wiley & Sons Ltd, 942 p.

Dalrymple, M.L., Hudson, I.L., and Ford, R.P.K., 2002, Finite mixture, zero-inflated Poisson and hurdle models with application to SIDS: Computational Statistics and Data Analysis, v. 41, p. 491-504.

Fisher, R., 1953, Dispersion on a sphere: Proceedings of the Royal Society of London, Series A, Mathematical and Physical Sciences, v. 217, p. 295-395.

Fitzharris, B.B., 1981, Frequency and climatology of major avalanches at Rogers Pass 1909-1977, DBR Paper956, National Research Council, Canadian Association Committee on Geotechnical Research, Ottawa, ON, 42 p.

Fitzharris, B.B., 1987, A climatology of major avalanche winters in western Canada: Atmosphere-Ocean, v. 25, p. 115-136.

Garrido, S., Santos, A.M.P., Santos, A.D., and Ré, P., 2009, Spatial distribution and vertical migrations of fish larvae communities off Northwestern Iberia sampled with LHPR and Bongo nets: Estuarine, Coastal and Shelf Science, v. 84, p. 463-475.

Genz, A., Bretz, F., Miwa, T., Mi, X., Leisch, F., Scheipl, F., and Hothorn, T., 2010, mvtnorm: Multivariate Normal and t Distributions: R package version 0.9-9. URL http://CRAN.R-project.org/package=mvtnorm.

Glazovskaya, T.J., 1998, Global distribution of snow avalanches and changing activity in the Northern Hemisphere due to climate change: Annals of Glaciology, v. 26, p. 337-342.

Greene, W., 1994, Accounting for excess zeros and sample selection in Poisson and negative binomial regression models: Working Paper EC-94-10, Department of Economics, New York University, 36 p.

Hachler, P., 1986, Analysis of the weather situations leading to severe and extraordinary avalanche situations, *in* Proceedings of the Davos Symposium, Davos, Switzerland, p. 295-304.

Hageli, P., and McClung, D.M., 2003, Avalanche characteristics of a transitional snow climate – Colombia Mountains, British Columbia, Canada: Cold Regions Science and Technology, v. 37, p. 255-276.

Hageli, P., and McClung, D.M., 2007, Expanding the snow-climate classification with avalanche-relevant information: initial description of avalanche winter regimes for southwestern Canada: Journal of Glaciology, v. 53, p. 266-276.

Hebertson, E.G., and Jenkins, M.J., 2003, Historic climate factors associated with major avalanche years on the Wasatch Plateau, Utah: Cold Regions Science and Technology, v. 37, p. 315-332.

Jackman, S., 2010, pscl: Classes and Methods for R developed in the Political Science Computational Laboratory, Stanford University: Department of Political Science, Stanford University, Stanford, California, R package version 1.03.3. URL http://pscl.stanford.edu/.

Kalnay, E., Kanamitsu, M., Kistler, R., Collins, W., Deaven, D., Gandin, L., Iredell, M., Saha, S., White, G., Woollen, J., Zhu, Y., Leetmaa, A., Reynolds, R., Chelliah, M., Ebisuzaki, W., Higgins, W., Janowiak, J., Mo, K.C., Ropelewski, C., Wang, J., Jenne, R., and Joseph, D., 1996, The NCEP/NCAR 40-year reanalysis project: Bulletin of the American Meteorological Society, v. 77, p. 437-470

Kistler, R., Kalnay, E., Collins, W., Saha, S., White, G., Wowllen, J., Chelliah, M., Ebisuzaki, W., Kanamitsu, M., Kousky, V., Dool, H.V.D., Jenne, R., and Fiorino, M., 2001, The NCEP-NCAR 50-Year Reanalysis: monthly means CD-ROM and documentation: Bulletin of the American Meteorological Society, v. 82, no. 2, p. 247-267.

McClung, D.M., 2002a, The elements of applied avalanche forecasting Part I: The human issues: Natural Hazards, v. 26, p. 111-130

McClung, D.M., 2002b, The elements of applied avalanche forecasting Part II: The physical issues and the rules of applied avalanche forecasting: Natural Hazards, v. 26, p. 131-146.

McCollister, C., Birkeland, K., Hansen, K., Aspinall, R., and Comey, R., 2003, Exploring multi-scale spatial patterns in historical avalanche data, Jackson Hole Mountain Resort, Wyoming: Cold Regions Science and Technology, v. 37, p. 299-313.

McCollister, C., 2004, Geographic knowledge discovery techniques for exploring historical weather rand avalanche data [Ms. thesis]: Bozeman, Montana State University, 106 p.

Mock, C.J., and Kay, P.K., 1992, Avalanche climatology of the western United States, with an emphasis on Alta, Utah: Professional Geographer, v. 44, p. 307-318.

Mock, C.J., and Birkeland, K., 2000, Snow avalanche climatology of the western United States mountain ranges: Bulletin of the American Meteorological Society, v. 81, p. 2367-2392.

Morrison, P., 2004, Orographic effects of winds at Stevens Pass ski area, *in* Proceedings, International Snow Science Workshop, Jackson Hole, Utah, USA, p. 232-238.

Myoung, B. and Deng, Y., 2009, Interannual variability of the cyclonic activity along the U.S. Pacific Coast: Influences on the characteristics of winter precipitation in the Western United States: Journal of Climate, v. 22, p. 5732-5747.

O'Hara, B.F., Kaplan, M.L., and Underwood, S.J., 2009, Synoptic climatological analyses of extreme snowfalls in the Sierra Nevada: Weather and Forecasting, v. 24, p. 1610-1624.

Perla, R. and Martinelli, M., 1978, Avalanche Handbook: Agricultural Handbook, 489, rev. ed., USDA Forest Service, Washington, D.C., 238 p.

Perry, L.B., Konrad, C.E., Schmidlin, T.W., 2007, Antecedent upstream air trajectories associated with northwest flow snowfall in the Southern Appalachians: Weather and Forecasting, v. 22, p. 334-352.

Plumer, M., Best, N., Cowles, K., and Vines, K., 2010, coda: Output analysis and diagnostics for Markov Chain Monte Carlo simulations: R package version 0.13-5. URL http://cran.r-project.org/web/packages/coda/index.html.

Purves, R.S., Morrison, K.W., Moss, G., and Wright, D.S.B., 2003, Nearest neighbours for avalanche forecasting in Scotland – development , verification and optimization of a model: Cold Regions Science and Technology, v. 37, p. 343-355.

Ramsey R.L. and Schafer, D.W., 2002, The Statistical Sleuth: A course in methods of data analysis, second edition: Pacific Grove, California, Duxbury, Thomson Learning, Inc. 742p.

Rocky Mountain Biological Laboratory, 2009, Long term monthly/yearly snow totals, accessed 5 April, 2010.
http://www.rmbl.org/home/index.php?module=htmlpages&func=display&pid=82.

Rogerson, P.A., 2006, Statistical methods for geography: A students guide: London, England, SAGE Publications Inc. 304 p.

Shepard, D., 1968, A two-dimensional interpolation function for irregularly-spaced data, *in* Proceedings of the 1968 Association for Computing Machinery National Conference, p. 517-524

Singh, A. and Ganju, A., 2004, A supplement to nearest-neighbour method for avalanche forecasting: Cold Regions Science and Technology, v. 39, p. 105-113.

Walker, M., Hall, A., Anderson, R.M. and Basañez, G., 2009, Density-dependent effects on the weight of female Ascaris lumbricoides infections of humans and its impact on patterns of egg production: Parasites and Vectors, v. 2, p. 1-18.

Welsh, A.H., Cunningham, R.B., Donnelly, C.F. and Lindenmayer, D.B., 1996, Modelling the abundance of rare species: statistical models for counts with extra zeros: Ecological Modelling, v. 88, p. 297-308.

Zeileis, A., Kleiber, C., and Jackson, S., 2008, Regression Models for Count Data in R: Journal of Statistical Software, v. 27, p. 1-25.